P-04-29

# Forsmark site investigation

# Interpretation of airborne geophysics and integration with topography

## Stage 1 (2002)

Hans Isaksson, Hans Thunehed, Mikael Keisu
GeoVista AB

February 2004

**Svensk Kärnbränslehantering AB**
Swedish Nuclear Fuel
and Waste Management Co
Box 5864
SE-102 40 Stockholm Sweden
Tel 08-459 84 00
+46 8 459 84 00
Fax 08-661 57 19
+46 8 661 57 19

ISSN 1651-4416
SKB P-04-29

# Forsmark site investigation

# Interpretation of airborne geophysics and integration with topography

## Stage 1 (2002)

Hans Isaksson, Hans Thunehed, Mikael Keisu
GeoVista AB

February 2004

*Keywords:* Airborne geophysics, Magnetics, Electromagnetics, Gamma-ray spectrometry, VLF, Lineament.

# Contents

# 1 Introduction

This document reports interpretation of airborne geophysics and integration with topography, which is one of the activities performed within the site investigation at Forsmark. The work was conducted according to activity plan AP PF-400-02-47 (SKB internal controlling document), by GeoVista AB; Hans Isaksson and Hans Thunehed. Mikael Keisu has been responsible for delivery of data.

The method descriptions “Metodbeskrivning för tolkning av flyggeofysiska data” (SKB MD 211.003) and “Metodbeskrivning för lineamentstolkning baserad på topografiska data” (SKB MD 120.001) are the principal frames of reference for the work. The document “Geological site descriptive model. A strategy for the model development during site investigations” /1/ is the main reference for the coordination of geophysical and topographical lineaments.

The main focus of the work was directed towards qualitative interpretations and a two dimensional description of the geophysical characteristics in relation to the bedrock geology. Issues concerning other disciplines, like quaternary geology, have not been addressed.

The work carried out during 2002–2003 comprises the first stage and a revision, stage 2, will be carried out after additional work during 2003–2004.

# 2 Objective and scope

The purpose of the interpretation of airborne geophysics and integration with topography is to describe areas with different geophysical properties and characteristics. Linear features, or lineaments, were given special attention, as they can provide important information on the extension of deformation zones in the bedrock. The work will form a basis for the geological bedrock mapping and future site descriptive models in the Forsmark area.

The work comprises:

- Processing and method specific interpretation of helicopter borne geophysical data.
- Coordination and linking of geophysical and topographical lineaments.

The method specific interpretation covers the whole helicopter borne survey area. However, the electrical properties of sea water makes the electromagnetic and VLF data somewhat unfavourable for structural interpretations and hence, the main focus in this stage, stage 1 (2002), will be on the mainland, where the coverage of data also is more complete.

A revision of the results, stage 2, will be carried out after further work during 2003–2004, that is; the geological mapping of the island areas, processing of the airborne EM data (inversion) and access to marine geological data that will provide better possibilities for lineament interpretation in the sea area.

# 3 Preparatory work

Collection of supportive data and some other preparatory work is needed for the processing, interpretation and evaluation of the helicopter borne geophysics.

The preparatory work comprises:

- Collection, processing and evaluation of the petrophysical data collected during 2002.
- Collection and in some cases processing of previous airborne geophysical data.
- Collection and preparation of other significant supportive information.

## 3.1 Petrophysical data

Sampling, statistical processing and evaluation of petrophysical data from 2002 have been reported by Mattsson et al /2/ and Isaksson et al /3/.

The purpose of petrophysical investigations is to gain knowledge of the physical properties of different rock types, thereby providing the basis for interpretation of, as in this case, airborne geophysical data.

## 3.2 Prior geophysical data and interpretations, version 0

Airborne geophysical surveys and interpretations in the Forsmark area have been used in previous work in the "Östhammar Feasibility study" /4/ and for the "Site descriptive model version 0" /5/, and provide information in a regional context.

### 3.2.1 Previous airborne magnetic data

A special emphasis has been put to improve the foundation for structural interpretation around the Forsmark power plant. The new helicopter borne survey could not cover the power plant area for safety and security reasons. The previous magnetic survey was partly influenced by an artificial magnetic source, originating from the construction of the Forsmark I power plant. By means of data processing, the effect of the artificial source has been minimized and the influence from the bedrock enhanced.

### 3.2.2 Data processing and results

The artificial magnetic anomaly consists of a positive maximum and a weaker minimum slightly to the north of the maximum (Figure 3-1). An attempt was made to fit a magnetic dipole field to these anomalies. However, this was not very successful. The sharp gradients indicate a shallow source and the distance between the maxima and the minima is too long to be compatible with a shallow dipole. Attempts were made to fit the anomalies to other analytical functions but with the same negative result. The conclusion from this modelling is that the magnetic anomaly source is dispersed and that the line spacing of the survey is too large to accurately describe this source.

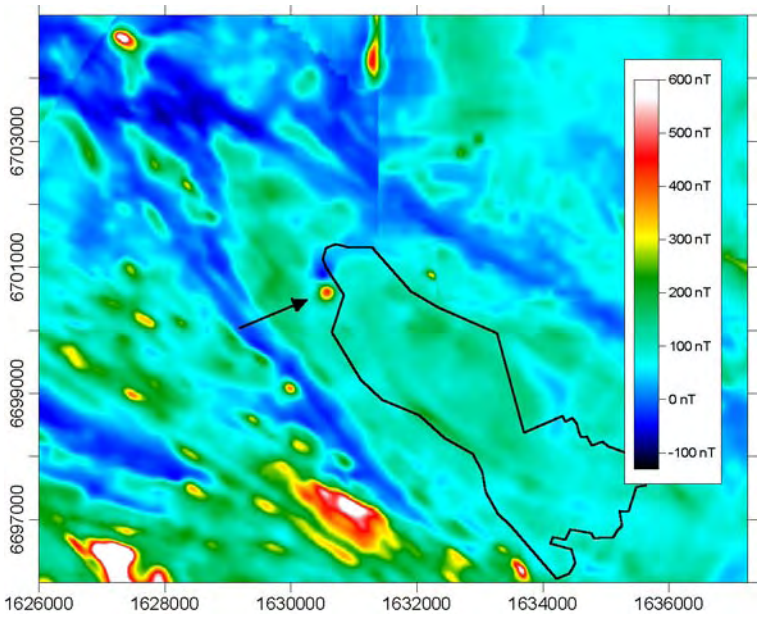


***Figure 3-1.*** *Mosaic of airborne magnetic surveys by SGU from 1976, 1982 and 1988 /5/. The arrow points at an artificial positive magnetic anomaly with a corresponding negative anomaly further north. Forsmark candidate area outlined with a solid black line.*

Those points that were obviously affected by the artificial anomaly were removed from the aeromagnetic data set. Such points appeared in four of the airborne survey profiles, which at this location have a SW-NE trend. This will produce a hole in the data coverage with a size of about 400 times 600 metres. Data from 3 km of the four profiles in question and one extra profile were extracted from the data set and a semivariogram was calculated (Figure 3-2). The purpose of this was to investigate the spatial correlation in the data to see if interpolation is justified to fill the hole in the data. Another purpose was to use the spatial statistics in Kriging interpolation. There will be a directional bias in the data pairs used to calculate the variogram since the data were collected along profiles. Some conclusions can still be drawn. There is a spatial correlation in the data up to distances of around 350 metres along the profiles and 700 metres perpendicular to the profiles. The anisotropy is around 1.7; directed perpendicular to the SW-NE profiles (cannot be estimated from the plots in Figure 3-2). These numbers imply that the spatial correlation is not really large enough to interpolate local, short wave-length features in the magnetic field in the area where data have been removed. Still, the correlation is strong enough to justify interpolation of broader trends, but the results should be used with some caution.

The magnetic field was interpolated in a 40 by 40 metres grid in the area of the outer square in Figure 3-3. The interpolation was performed with the Kriging method using Surfer v.8 and the variogram model from Figure 3-2. A smooth transition between this grid and the larger original grid was achieved by combining them as a weighted average. The weights of the new grid and of the old grid were 1.0 and 0.0 respectively inside the inner square in Figure 3-3 and the reverse weights were applied outside the outer square. A linear transition was applied in between. The result should be compared to Figure 3-1.

Figure 3-4 shows an example of the edited, airborne magnetic data presented as a RGB colour composite of magnetic total field (red), 1: st vertical derivative (green) and horizontal derivative (blue). This data has been used in the structural interpretation, Chapter 4, compare also with Figures 4-3 and 4-4.

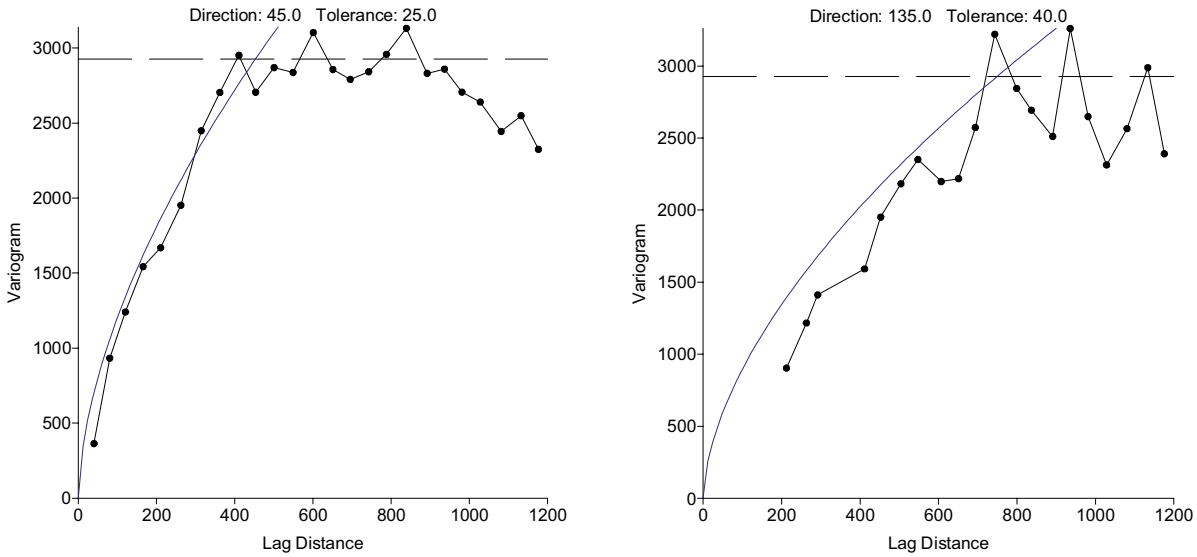


***Figure 3-2.*** *Semivariograms calculated from aeromagnetic data from five profiles around the artificial anomaly in Figure 3-1. The left graph shows the result of data pairs in SW-NE direction whereas the right graph shows the result of data pairs in SE-NW direction. The solid line corresponds to a power-law anisotropic variogram model used for interpolation. The dashed black lines correspond to the data variance.*

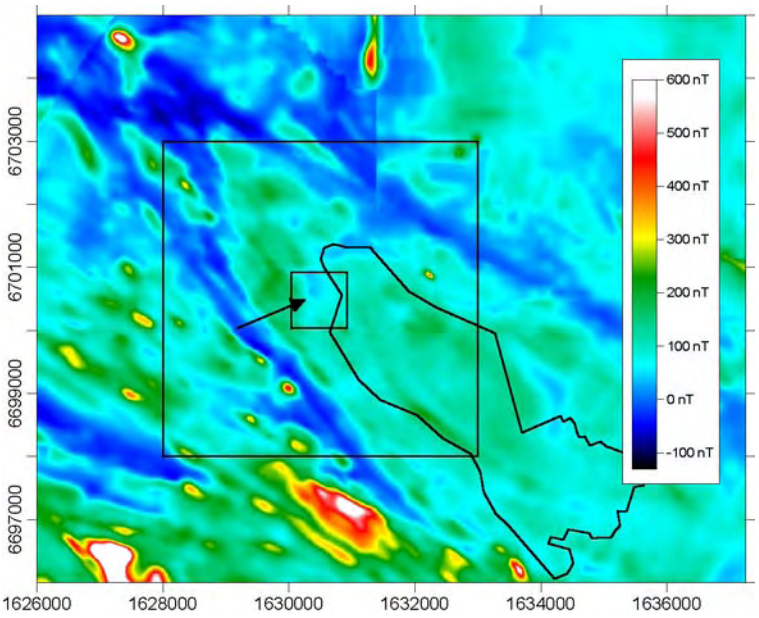


***Figure 3-3.*** *Result of weighted average of existing grid and a new grid resulting from Kriging interpolation of data where anomalous magnetic values caused by the artificial source have been removed. See text for details about weighting.*

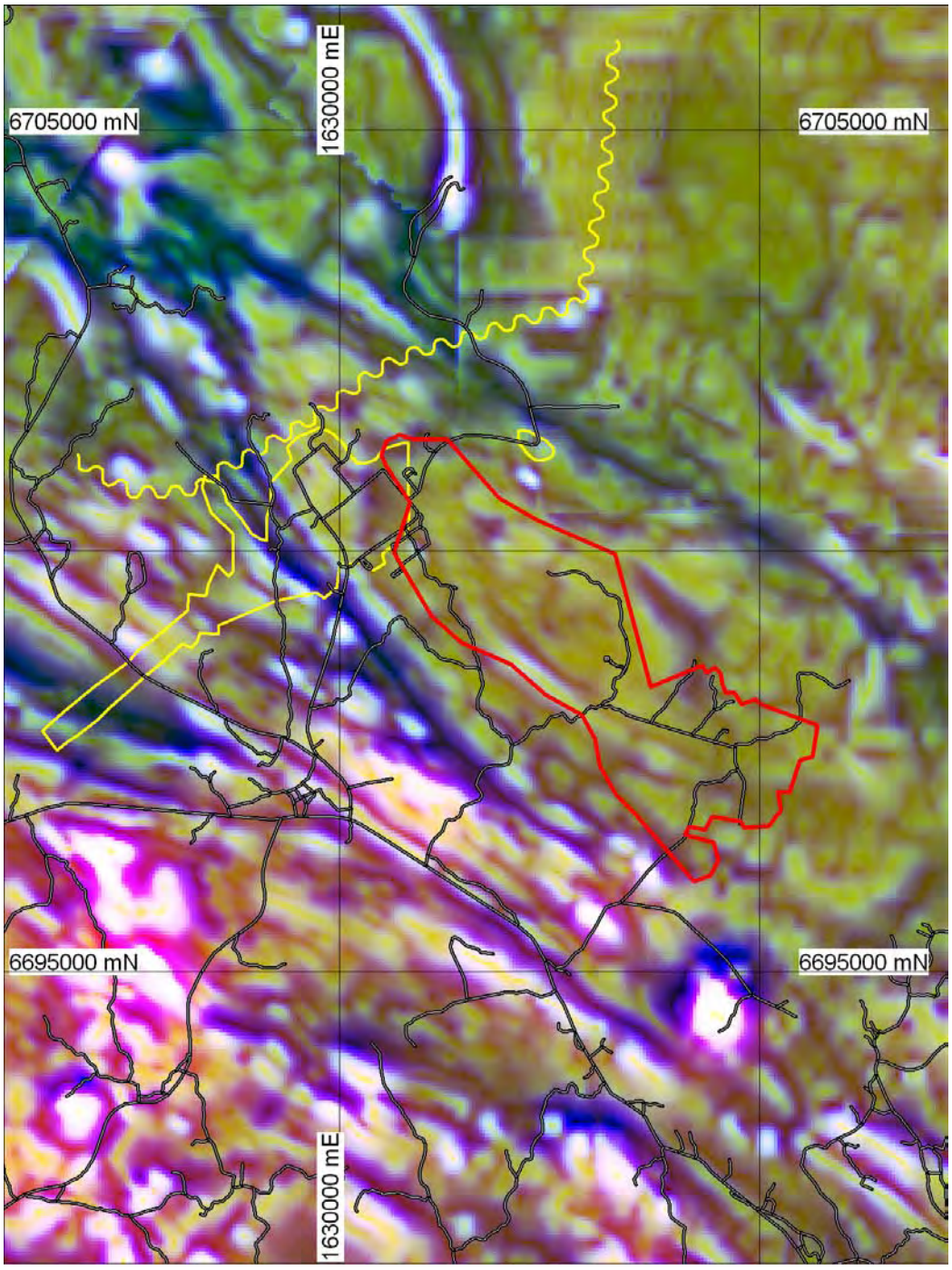


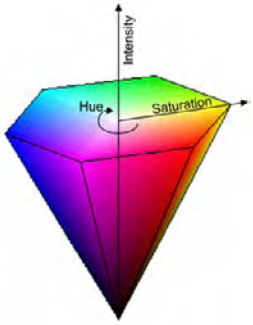


| ***Colour*** | ***Element*** |
|---|---|
| *Red* | *Magnetic total field* |
| *Green* | *Magnetic 1: st vertical derivative* |
| *Blue* | *Magnetic horizontal derivative* |

*Hue and saturation describes the relative distribution of the variables. Dark and bright colours indicate low and high intensity, respectively.*

***Figure 3-4.*** *Airborne magnetics, edited, presented as a RGB, colour composite. Forsmark candidate area outlined with a red line. Yellow markers outline artificial, disturbed areas during the most recent survey 2002. Also compare with Figures 4-3 and 4-4.*

## 3.3 Other supportive information

Other supportive information used during the interpretation are geographical GIS-data, infrared orthophoto data, outcrop information, elevation data as well as geology and lineaments from the site descriptive model version 0 /5/.

A special emphasis has been put to find geographical information that describes sources that can produce artificial geophysical anomalies, i.e. electrical installations like power lines, telephone cables, large iron or steel objects, etc. When artificial sources is suspected, the new helicopter survey data has also been compared with older airborne geophysical data to see if the anomaly appears on both data sets.

# 4 Interpretation of helicopter borne geophysical data

During August and September, 2002, geophysical measurements from helicopter were carried out in the Forsmark area by the Geological Survey of Norway /6/.

The present work comprises further processing and interpretation of the airborne magnetics, electromagnetics (EM), VLF and gamma ray spectrometry data. The interpretation is performed according to procedures and methodology described in the method description "Metodbeskrivning för tolkning av flyggeofysiska data" (SKB MD 211.003) and activity plan AP PF 400-02-47 (SKB internal controlling document). This work is the first stage, covering mainly the mainland area, and the interpretation has been qualitative and two-dimensional (surface mapping).

The interpretation result forms a basis for the bedrock mapping, "Berggrundskartering vid Forsmark, 2002–2003", activity plan AP PF 400-02-11 (SKB internal controlling document), and will also form part of future site descriptive models.

The interpretation has covered the whole airborne survey area. However, it must be noted that the airborne EM and VLF data give rather limited possibilities to delineate structures in the sea area, see also Chapter 4.3.2. Further processing of the airborne EM data (inversion) as well as access to marine geological data will provide better possibilities for future lineament interpretations and co-ordination of lineaments in the sea area.

All work has been performed using Windows based computers and software, see Table 4-1. The results of the interpretation have been delivered to SKB in ArcView format, and the data can be extracted from SKB's GIS database, see Chapter 8.

**Table 4-1. Software that has been used in this study.**

| Software | Trademark | Activity |
|---|---|---|
| Geomatica | PCI | Image processing and "on screen" interpretation |
| Surfer | Golden Software Inc | Grid processing, presentations |
| Oasis | Geosoft Inc | Grid filtering and transformations |
| MapInfo | MapInfo Inc | Documentation of characteristics. Map production. Presentations |
| ArcView | ESRI | Delivery format |
| In-house | GeoVista | AGC transformation of airborne EM data |

## 4.1 Input data

The helicopter borne geophysical survey /6/ comprised multi-frequency electromagnetic (EM) measurements, magnetometry and gamma-ray spectrometry. VLF-measurements were included as an option when suitable VLF-transmitters were operating. Measurements were performed within a larger area with north-south flight direction and within a smaller area with east-west flight direction. The line spacing was in both cases 50 metres. Tie lines were flown every 500 metres in both directions. The data coverage can be seen in Figure 4-1.

The nominal flight altitude of the helicopter was 60 metres although the pilot had to ascend over e.g. power lines and high trees. The magnetometer and the EM system were placed in a bird that was towed 30 metres below the helicopter. The VLF sensor was placed along the wire connecting the bird to the helicopter whereas the spectrometer crystals were placed on the helicopter itself. Details about the instrumentation and the pre-processing of the data can be found in /6/. A short description is given below. In order to save time, preliminary data were used for parts of the interpretation. However, this has not affected the final results.

There are rather extensive artificial disturbances in the Forsmark area and the most important sources; the nuclear power plants, the power lines and the DC-cable, are outlined in a GIS-layer for overlay during the work and for presentations, see Figure 4-3, 4-4 and 4-5.

### *Magnetometry*

Magnetic measurements were performed with a sampling rate of 0.1 seconds giving a measurement spacing of around 3 metres. The contractor provided a base station magnetometer for diurnal corrections. However, the DC power line within the survey area affected the base station readings and data from the SGU observatory at Fiby were used instead. The effect of varying current in the DC cable was, as far as possible, corrected for by SGU /7/. A map of the magnetic total field is presented in Figure 4-2.

### *EM*

The EM system consists of coils transmitting in five frequencies and corresponding receiver coils. The secondary magnetic field was recorded with a sampling rate of 0.1 seconds. The frequencies are 980 and 7001 Hz coaxial coils and 880, 6606 and 34133 Hz coplanar coils. The helicopter ascended at regular intervals to ground effect free altitude to enable estimates of instrument drift.

### *Spectrometry*

Gamma-ray spectrometry was measured with a receiver crystal placed on the underside of the helicopter. An upward looking crystal was also used. The integration time and sampling rate of the instrumentation was 1 second giving a measurement spacing of around 30 metres. The raw spectral data were transformed to equivalent grades of K, Th and U (at ground surface) after corrections for radon, cosmic radiation and altitude attenuation.

### *VLF*

VLF-measurements were performed with one inline and one orthogonal sensor. The method was included as an option and lack of operating VLF-transmitters was not allowed to cause delays. However, the data coverage was almost the same as for the other methods (Figure 4-1) although different VLF-transmitters had to be used for different flights. The sampling rate for VLF-measurements was 0.2 seconds.

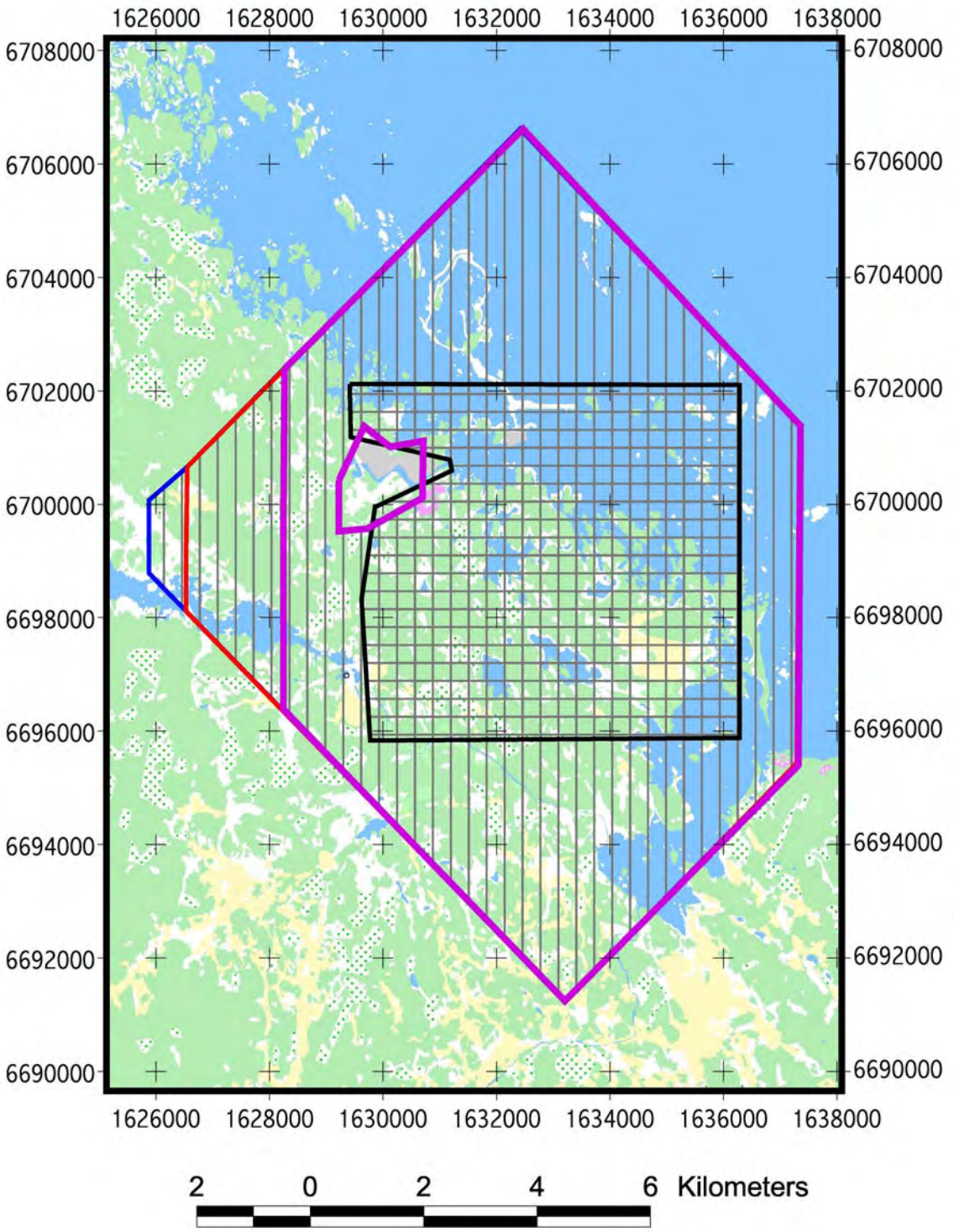


***Figure 4-1.*** *Map showing data coverage of the different methods in the helicopter borne survey, NGU 2002 /6/. Violet: VLF NS lines, red: EM and magnetometry NS lines, blue: Spectrometry NS lines, black: All methods EW lines. No data have been acquired around the nuclear power plant.*

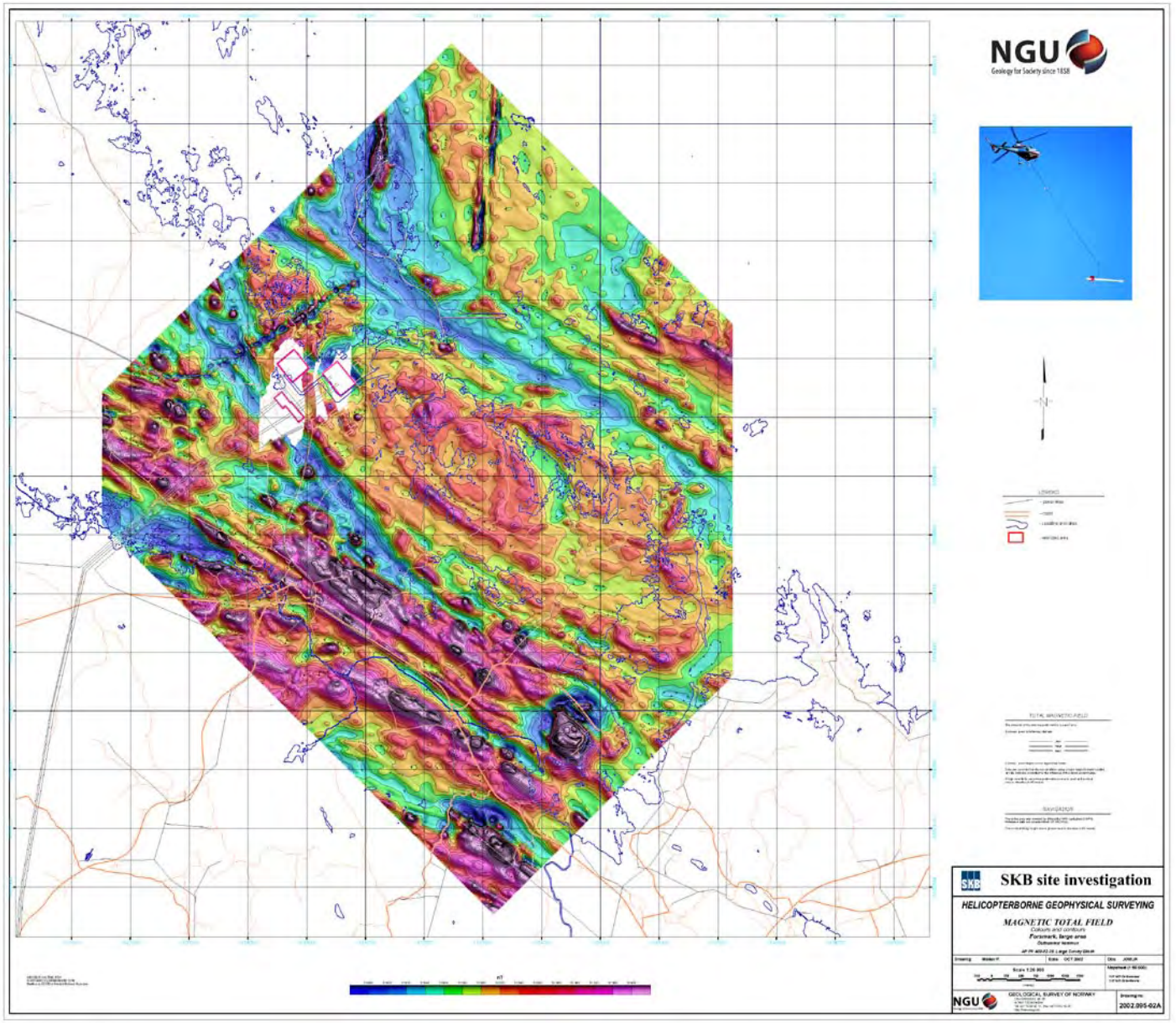


***Figure 4-2.*** *Magnetic Total Field, North-South survey area. Map showing the magnetic data from the helicopter borne survey, NGU 2002 /6/, also corrected for the effect from the DC power line /7/. Note the lack of data around the Forsmark nuclear power plant.*

## 4.2 Magnetics

### 4.2.1 Data processing

The magnetic total field, recorded during the helicopter survey, has been interpolated to a 10 × 10 m grid, by means of a linear Kriging routine (Surfer 8 – ™ Golden Software), with a search radius of 125 m and 55 m, perpendicular to and along the flight direction respectively. The two survey direction has been interpolated separately and treated as individual data sets.

A large number of filtering and transformations (Oasis – ™ Geosoft Inc), has been executed on the two datasets.

- 1:st and 2:nd vertical derivative,
- horizontal derivative along and perpendicular to the flight direction,
- total horizontal derivative,
- transformation to X-,Y- and Z-component and total horizontal field,
- derivative of each of the components; dX,dY,dZ,dH,
- analytical signal,
- Sobel transformation,
- pseudo gravity integration and derivatives,
- susceptibility mapping,
- automatic gain control,
- high pass filtering.

When applicable, reduction to the pole and/or upward continuation has been performed prior to, or has been included in the filtering. The same is valid for IGRF-correction which in some transformations is needed for further processing. After interpolation and filtering, the data was visually inspected, by means of image analysis (Geomatica – ™ PCI), for the most useful data layers intended for the structural interpretation. The most useful layers for the structural interpretation proved to be:

- Magnetic total field.
- 1:st and 2:nd vertical derivatives.
- Total horizontal derivative.

An example of the processing result is presented in Figure 4-3 and 4-4, for the NS and EW survey direction respectively.

A stacked profile presentation of the magnetic total field has also been produced as a vector layer to support the interpretation work. The previous airborne magnetic data covering the Forsmark area have also been used, mainly in the areas disturbed by artificial sources; see Chapter 3.2 and Figure 3-4.

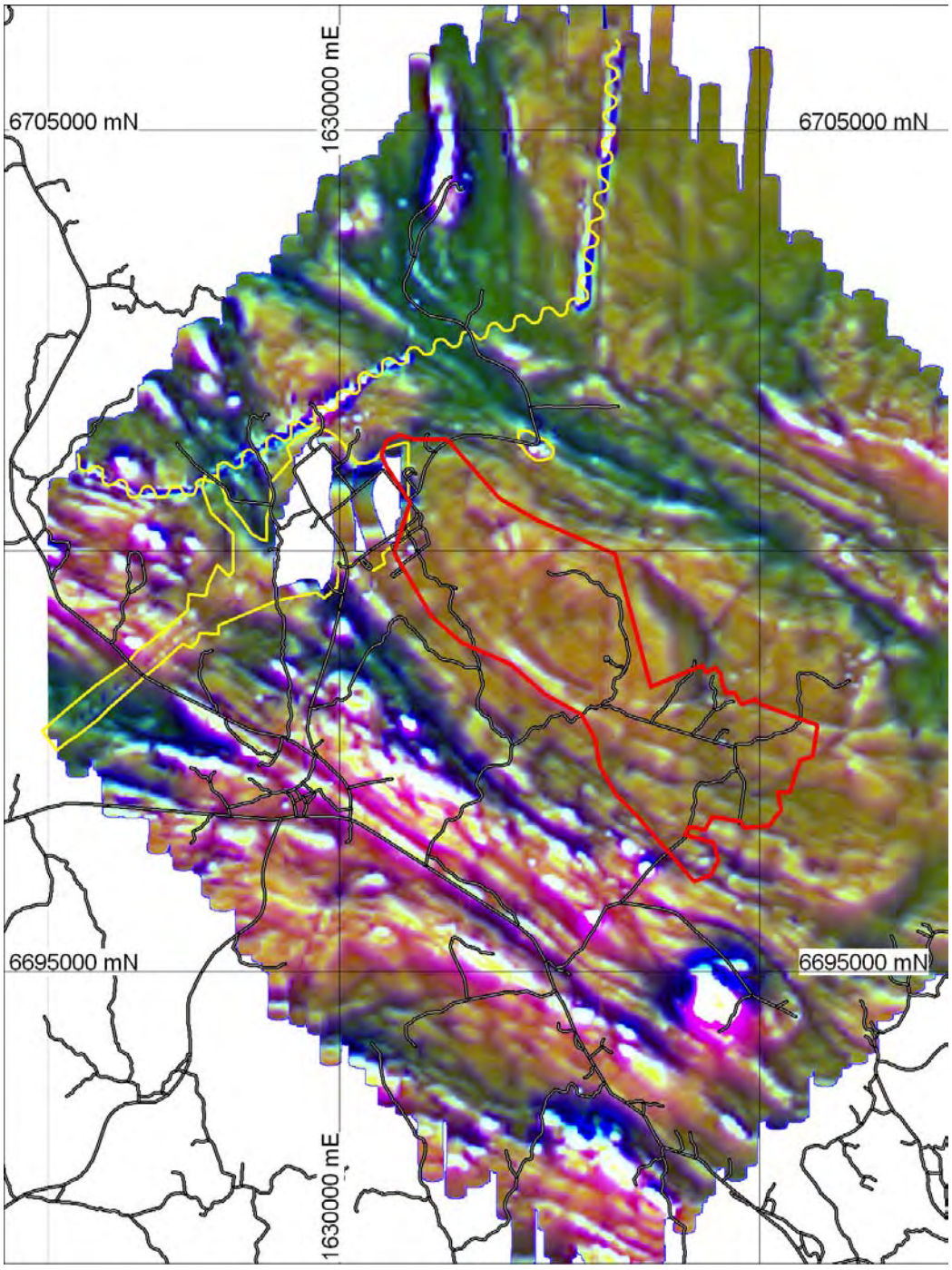


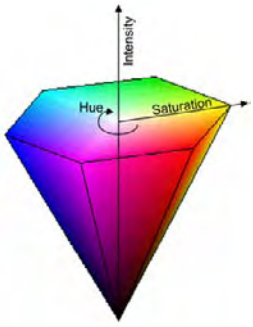


| ***Colour*** | ***Element*** |
|---|---|
| *Red* | *Magnetic total field* |
| *Green* | *Magnetic 1: st vertical derivative* |
| *Blue* | *Magnetic horizontal derivative* |

*Hue and saturation describes the relative distribution of the variables. Dark and bright colours indicate low and high intensity, respectively.*

***Figure 4-3.*** *Airborne magnetics, NS-survey, presented as a RGB, colour composite. Forsmark candidate area outlined with a red line. Yellow markers outline artificial, disturbed areas.*

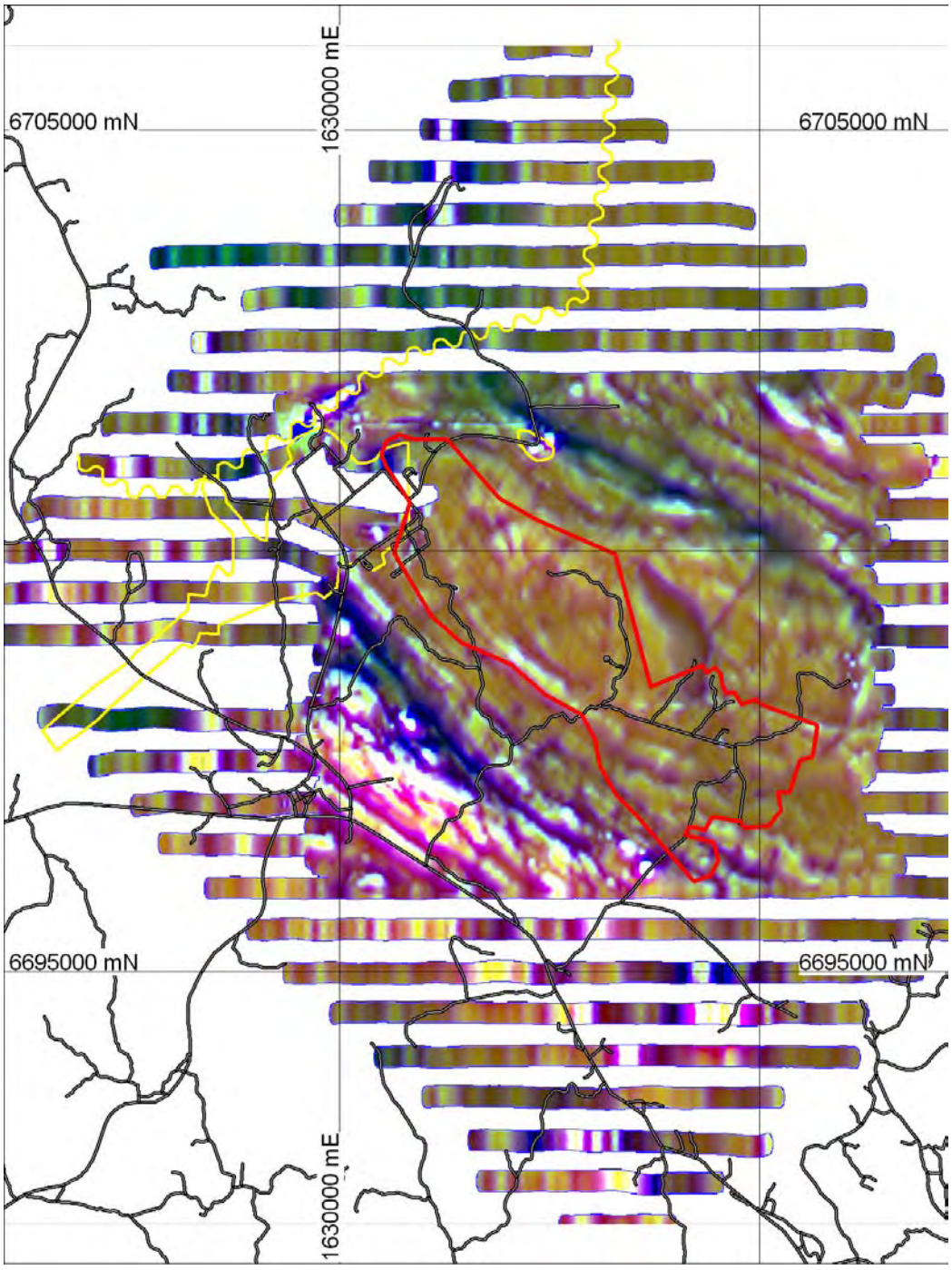


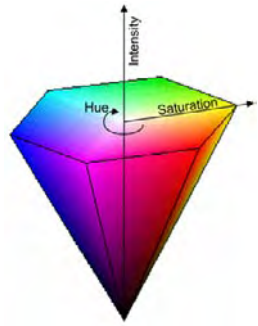


| ***Colour*** | ***Element*** |
|---|---|
| *Red* | *Magnetic total field* |
| *Green* | *Magnetic 1: st vertical derivative* |
| *Blue* | *Magnetic horizontal derivative* |

*Hue and saturation describes the relative distribution of the variables. Dark and bright colours indicate low and high intensity, respectively.*

***Figure 4-4.*** *Airborne magnetics, EW-survey, presented as a RGB, colour composite. Forsmark candidate area outlined with a red line. Yellow markers outline artificial, disturbed areas.*

### 4.2.2 Results

The interpretation has been carried out by visual identification, delineation and characterization of structural features, using image analysis (Geomatica – ™ PCI) and GIS-techniques (Mapinfo – ™ Mapinfo).

#### *Anomaly pattern*

The interpretation is divided into two phases. The first one is to discriminate areas with different structural magnetic anomaly patterns or texture. This is commonly used to differentiate between supracrustal rocks with a banded pattern and intrusive rocks with an irregular pattern. Beside texture, the magnetic patterns are also classified into low, medium, high and very high magnetization. In areas with low magnetization, the anomaly pattern is difficult to define. Magnetic maxima connections are outlined as possible magnetic bands to support the interpretation of the structural geological setting. A special emphasis has been put to identify magnetic connections with a strong anomaly appearance. These features possibly indicate magnetite mineralizations, and in some cases they correspond, spatially, to known Fe-occurrences. Usually, also dyke like anomalies can be identified in the magnetic field. However, in spite of the high spatial resolution, no such anomaly has been noted in the Forsmark area.

Figure 4-5 shows the result of both the anomaly pattern and the lineament interpretation of the airborne magnetic data. Sources of artificial disturbances in the Forsmark area, like the nuclear power plants, power lines and the DC-cable, are also outlined, see the yellow overlay in Figure 4-1, 4-3 and 4-4.

Of special interest is to mention the magnetic pattern close to and within the Forsmark candidate area. Most of the area shows an irregular pattern with medium magnetic magnetization, but within this class a low magnetic pattern occurs. Investigation of the rock parameters /3/ shows that the metagranite-metagranodiorite group in general has a moderate magnetic susceptibility, 0.004–0.01 SI, and a tail into very low magnetic susceptibility. These features will need further follow up during the geological mapping 2003.

Of interest is also that the same rock type, metagranite-metagranodiorite, shows a somewhat higher magnetization from the Forsmark power plants and further to the NW and forms the NW part of the Forsmark tectonic lens. This feature is also clearly separated to the SE by a low magnetic pattern indicating a flexure structure.

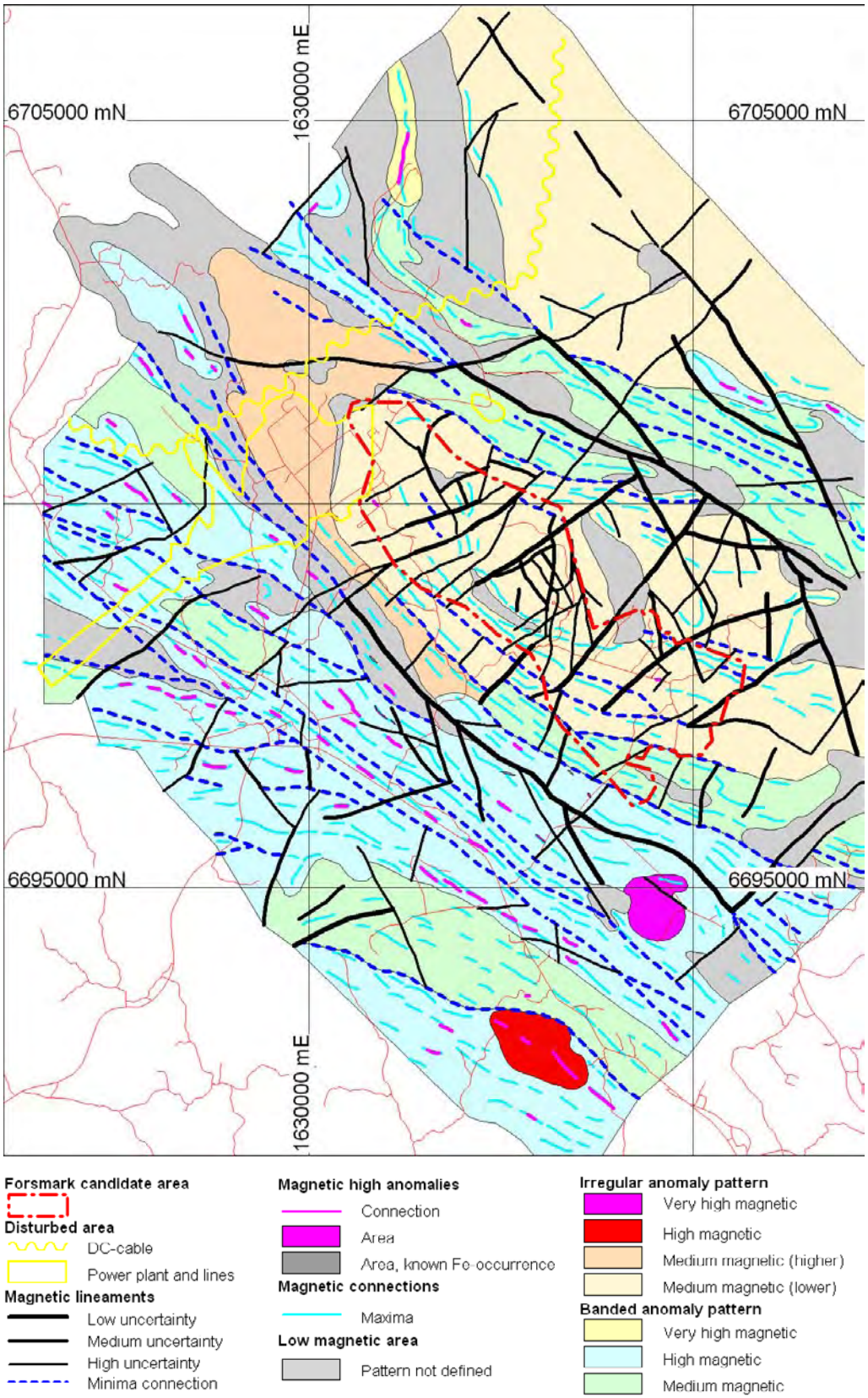


***Figure 4-5.*** *Airborne magnetic, structural interpretation. The Forsmark candidate area is outlined with a red dot-dashed line. Yellow markers show artificial, disturbed areas. The areas with known Fe-occurrences can be difficult to see in this scale of presentation.*

### *Lineament identification*

The second interpretation phase is to identify linear features which can be represented by lineaments as magnetic minima and other linear dislocations in the magnetic field. The lineaments are graded in low, medium and high uncertainty with respect to the clarity in which they appear.

The structural geology in the Forsmark area is characterized by a rather strong ductile deformation of both supracrustal and intrusive rocks and hence, also intrusive rocks often show a rather strong banded component in the magnetic pattern. Magnetic connections that appear as minima parallel to the general bedrock structures are difficult to judge as being lineaments or low magnetic rock types. In this work they are identified as potential fracture zones and, hence, noted as lineaments with a separate denomination of magnetic “minima connection”.

The magnetic total field mainly contributes information about the bedrock and the influence by the overburden is generally small. Hence, the interpretation yields similar information both on the mainland and on the sea area.

In total, 247 magnetic lineaments have been identified. Based on the attached attribute table, Table 4-3, some general statistical results are presented, see Table 4-2.

The interpretation results are stored in GIS-format and each of the units identified has an attribute table attached, see also Table 4-3.

The presence and distribution of magnetic lineaments is somewhat different within different parts of the investigated area. The area SW of the Forsmark candidate area is dominated by a very strongly elongated ductile deformation which makes it more difficult to identify brittle structures. The candidate area shows a rather distinct and gently folded magnetic pattern, the magnetization level is moderate and hence, discordances and linear minimum are more easily identified. The area immediately NE of the candidate area is again affected by strong ductile deformation and further to the NE, the rocks shows a low magnetization which makes it more difficult to identify lineaments.

The central area of investigation, including the candidate area, is also covered by two survey directions, Figure 4-1. The EW flight direction, Figure 4-4 makes it easier to identify structures with a NS extension, that is, approximately NS ± 30°.

Figure 4-6 a and c show the magnetic data over the candidate area, strongly enhanced using the magnetic analytical signal, vertical and horizontal derivative. For each of the survey directions the identified lineaments are overlaid in Figure 4-6 b and d to show the lineament appearance in the data and the foundation for the interpretation. The line thickness indicates the level of uncertainty, that is, thin-thick lines equals high-low uncertainty. In general, more lineaments are identified within the candidate area but they also show a higher degree of uncertainty. Figure 4-7 a and b show the identified magnetic lineaments on top of the topographic map in the NW and SE part of the candidate area, respectively.

**Table 4-2. Compilations of some attribute information for magnetic lineaments. Figures show number of occurrences.**

| Character | Low uncertainty | Medium uncertainty | High uncertainty | Total number |
|---|---|---|---|---|
| Minima | 27 | 47 | 100 | 174 |
| Minima connection | 16 | 53 | 4 | 73 |
| Total | 43 | 100 | 104 | 247 |

**Table 4-3. Attribute table for structural magnetic anomaly interpretation.**

| Field name | Name | Description | Attribute used to describe anomaly patterns | Attribute used to describe magnetic lineaments |
|---|---|---|---|---|
| Id_t | Identity | Identity of the anomaly pattern | Not assigned in this work | Not assigned in this work |
| Origin_t | Origin | Major type of basic data | Magnetics | Magnetics |
| Class_t | Classification | Classification of the anomaly pattern | Not assigned in this work | Not assigned in this work |
| Method_t | Method | The type of data in which the observation is identified | Magnetic 10m grid | Magnetic 10m grid |
| Char_t | Character | Character of the observation | Banded or irregular pattern. Very high, high, medium (low and high) or low magnetic intensity. Connection. | Minimum, minima connection |
| Uncert_t | Uncertainty | Gradation of identification, in terms of uncertainty | Low/Medium/High | Low/Medium/High |
| Comment_t | Comment | Specific comments to the observation | | |
| Process_t | Processing | Data processing performed | Filtering, image analysis | Filtering, image analysis |
| Date_t | Date | Point of time for interpretation | 20030412 | 20030411 |
| Scale_t | Scale | Scale of interpretation | 20000 | 20000 |
| Platform_t | Platform | Measuring platform for the basic data | Airborne, 50m altitude | Airborne, 50m altitude |
| Width_t | Width | Width on average | Not assigned in this work | Not assigned in this work |
| Precis_t | Precision | Spatial uncertainty of position | 10–100m, 20m in general | 10–100m, 20m in general |
| Sign_t | Signature | Work performed by | hi (Hans Isaksson), GeoVista AB | |

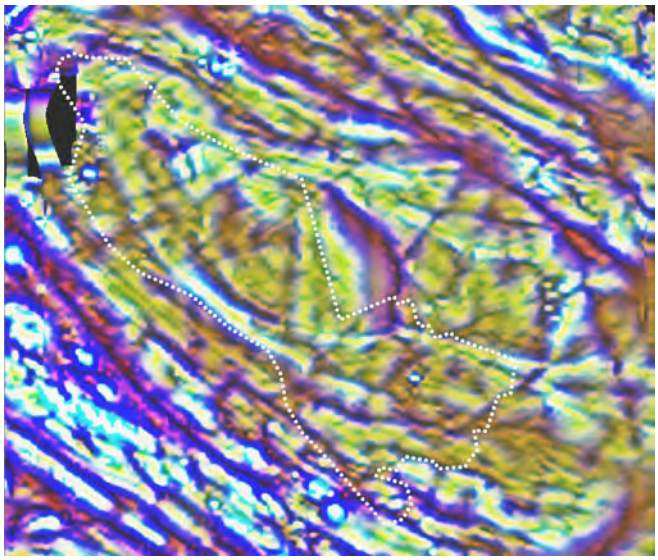

*Figure 4-6 a).*

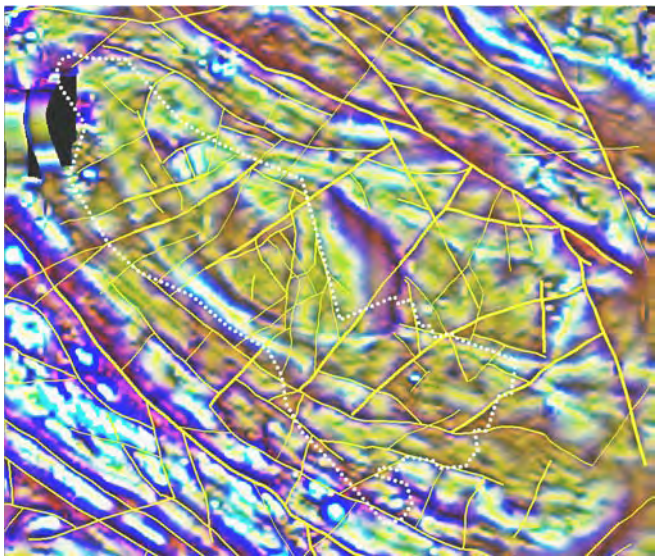

*Figure 4-6 b).*

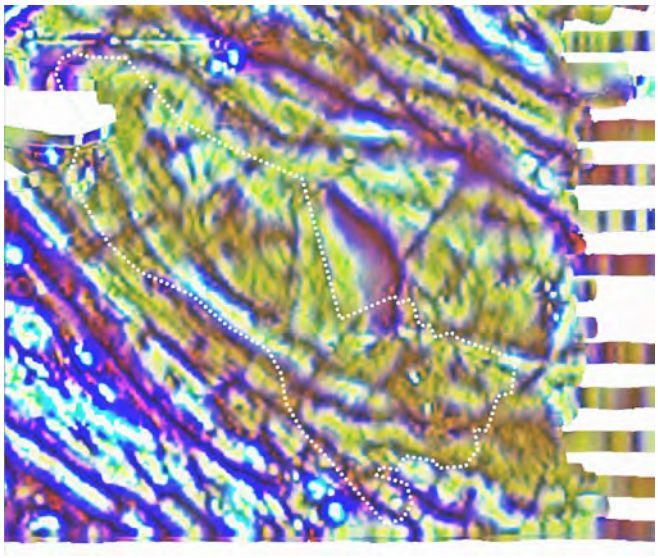

*Figure 4-6 c).*

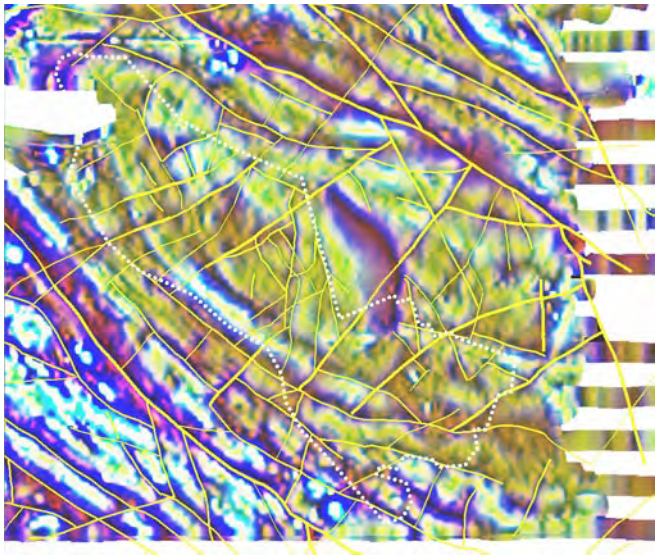

*Figure 4-6 d).*

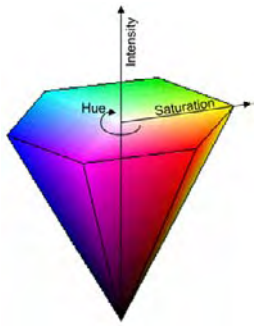


| ***Colour*** | ***Variable*** |
|---|---|
| *Red* | *Magnetic analytical signal* |
| *Green* | *Magnetic 1:st vertical derivative* |
| *Blue* | *Magnetic horizontal derivative* |

*Hue and saturation describes the relative distribution of the magnetic variables. Dark and bright colours indicate low and high intensity, respectively.*

***Figure 4-6.*** *Contrast enhanced airborne magnetics over the Forsmark candidate area, a-b) the NS-survey and c-d) the EW-survey, presented as a RGB, colour composites, with and without lineament overlay. The candidate area is outlined with a dotted black line. Magnetic lineaments are outlined in yellow. thick-thin lines indicate low-high uncertainty, respectively.*

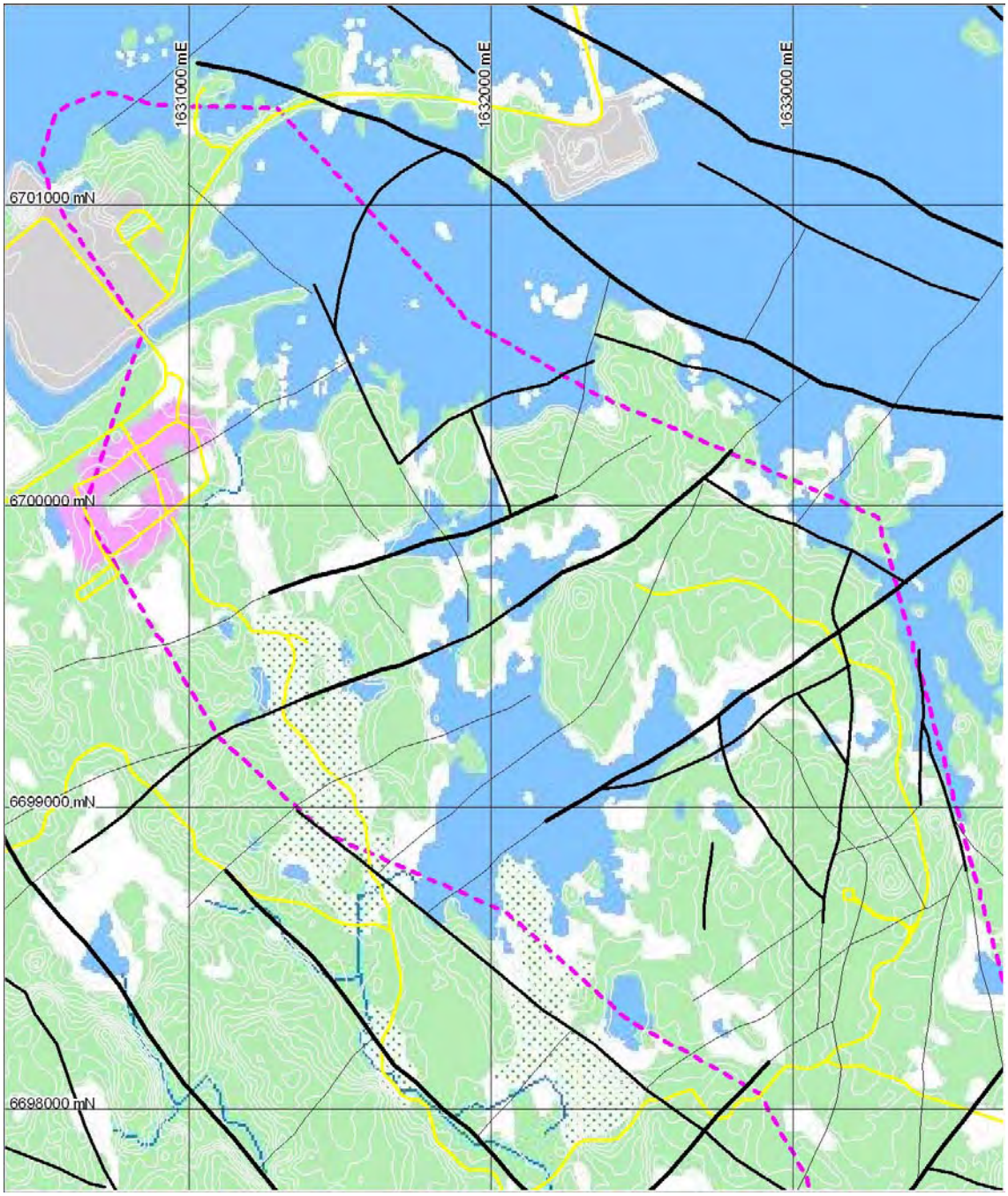


***Figure 4-7 a.*** *NW part of the Forsmark candidate area, outlined with a dotted magenta line. Magnetic lineaments outlined as solid black lines. Thick –> thin lines indicates low –> high uncertainty, respectively.*

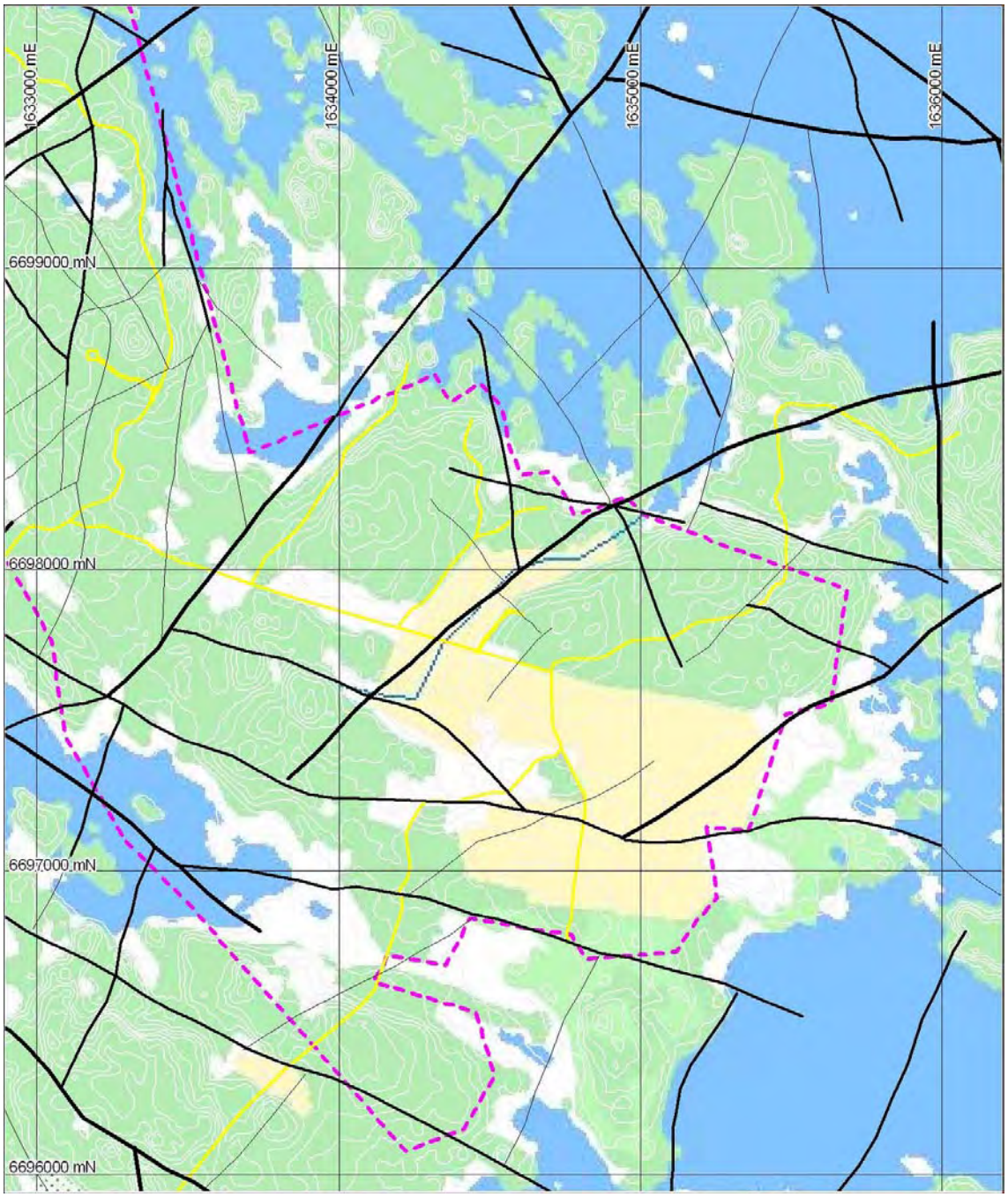


***Figure 4-7 b.*** *SE part of the Forsmark candidate area, outlined with a dotted magenta line. Magnetic lineaments outlined as solid black lines. Thick –> thin lines indicates low –> high uncertainty, respectively.*

#### *Uncertainties*

Basically, lineaments are graded in low, medium and high uncertainty with respect to the clarity in which they appear. However, also some other specific uncertainties can be pointed out regarding magnetic lineaments and their character.

A discrete, linear low magnetic feature with a discordant appearance in the magnetic pattern often originates from fracture zones in the bedrock. However, in the Forsmark area, with the strong ductile and elongated deformation pattern it can be difficult to distinguish between a concordant, narrow rock type with low magnetization and a lineament caused by a fracture zone.

Differences in overburden thickness also give different conditions for lineament identification. Large areas with a thin overburden give a better spatial and dynamic resolution of the magnetic pattern and hence, lineaments are more easily identified.

Topographical subsurface features like narrow depressions in the bedrock surface can give rise to a locally deeper overburden and hence, also cause a linear magnetic low, not necessarily corresponding to changes in bedrock susceptibility due to fracturing.

Horizontal to sub-horizontal structures are more difficult to identify in the magnetic field and when they occur they often appear as curved structures.

## 4.3 EM

### 4.3.1 Data processing

The EM data from Forsmark suffered from noise induced by power lines and other man-made installations. This resulted in more or less random noise close to the major power lines but also as irregular level shifts for two of the system frequencies (7 kHz coaxial coils and 34 kHz coplanar coils). These level shifts appear more or less over the entire survey area and so often and with such magnitude that they seriously reduce the information that can be extracted from measurements with these two frequencies. Fortunately, the level shifts are correlated so that when a shift appears in one frequency, a corresponding shift appears on the other. Also, the shifts appear with comparable magnitudes for both the in-phase and quadrature components. Based on this observation, an effort was made to reduce the influence of such noise.

Transformation into principal components (PC's) is a technique where multivariate data are transformed into components that are uncorrelated to each other. A PC is calculated as a linear combination of the original components. PC transformation can be seen as a rotation of the coordinate system so that the coordinate axes take the principle directions of the data distribution in multivariate space. With a certain number of original components there will be the same number of PC's where the first one will correspond to a coordinate axis along the direction of maximum variance (and hence maximum correlation) in the data. The higher order PC's will gradually explain less of data variance (and correlation). The last PC will, in general, mainly contain uncorrelated random noise.

Since the level shifts in the two frequencies are correlated to each other but uncorrelated to the other frequencies it was possible to extract them as a PC. In theory it should be possible to blank this PC and then make an inverse transformation back to the original data components. However, with real data some of the noise will leak to other PC's and the shifts would only be reduced by around 60 to 90%. Instead, by visual inspection the

"level-shift-PC" was weighted and then directly subtracted from the original components. An example of the results of such processing can be seen in Figure 4-8. This had to be done on a flight by flight basis since the relative magnitudes of the level shifts varied. It is inevitable that real anomalies to some degree will be distorted with this kind of data processing. However, this distortion was in general quite moderate and has mainly affected large anomalies, caused by sea water, in the coaxial-coil components.

The data were filtered gently with a median filter and then transformed into the PC domain once more. Most of the true anomalies will show up in the low order PC's since data components are correlated to each other. The PC's were then median and average filtered where the filter length was kept short for the low order PC's and longer filters were used for the higher order PC's. The actual length of the filters were interactively adjusted to the data quality, where longer filters were used e.g. for noisy data obtained close to the major power lines.

The filtered data were levelled by using the readings at high altitude that were made at regular intervals during the flights. Such readings were fitted to low-order polynomials that were subtracted from the data. The polynomial order was selected interactively where the result was inspected on a computer monitor before approval. Filtered and levelled data were finally cut into profiles.

When inspecting profiles and comparing with image maps based on interpolated data grids it became evident that many subtle anomalies were difficult to detect in the maps. Minor fracture zones are expected to cause such subtle anomalies. The data were therefore processed with automatic gain control (AGC) to enhance the appearance of subtle anomalies. A window length has to be selected when performing AGC. This was set to 6 seconds of recording, corresponding to a profile length of around 180 metres. Anomalies wider than the window will be attenuated. Most wide anomalies will however be detected in the original data. Narrow anomalies where the strike direction make a small angle relative the profile will inevitable be attenuated by AGC. However, this is not a problem for the central part of the survey area, since it is covered by data from two flight directions. The AGC was calculated as:

$$AGC = \frac{in - ave(in)}{\left(\frac{1}{N} \cdot \sqrt{SS}\right)^{0.75}}$$

where

AGC = AGC filtered output
in = input data
ave(in) = average of input data in AGC window
N = number of samples in AGC window

and

$$SS = \sum_{i-1}^{N} \left(in_i - ave(in)\right)^2$$

An interpretation of lineaments was performed where apparent resistivity data from the contractor and AGC-filtered data were used as input data. Interpolated grids were used to produce colour and greyscale image layers. Including all frequencies and both survey directions this means that a total of 24 image layers were used. Additionally, the levelled secondary field data were used to check some anomalies. Examples of some of the most relevant image layers are seen in Figures 4-9 to 4-11.

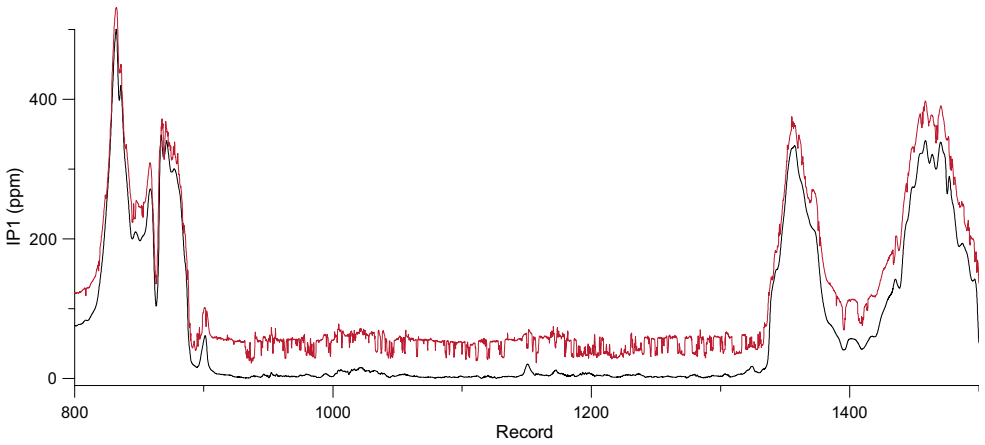


***Figure 4-8.*** *Raw data of in-phase component of 7 kHz, coaxial components (red curve). The same data after level shift reductions, PC-domain filtering and levelling with high-altitude readings (black line). Flight 22. One record corresponds to one second.*

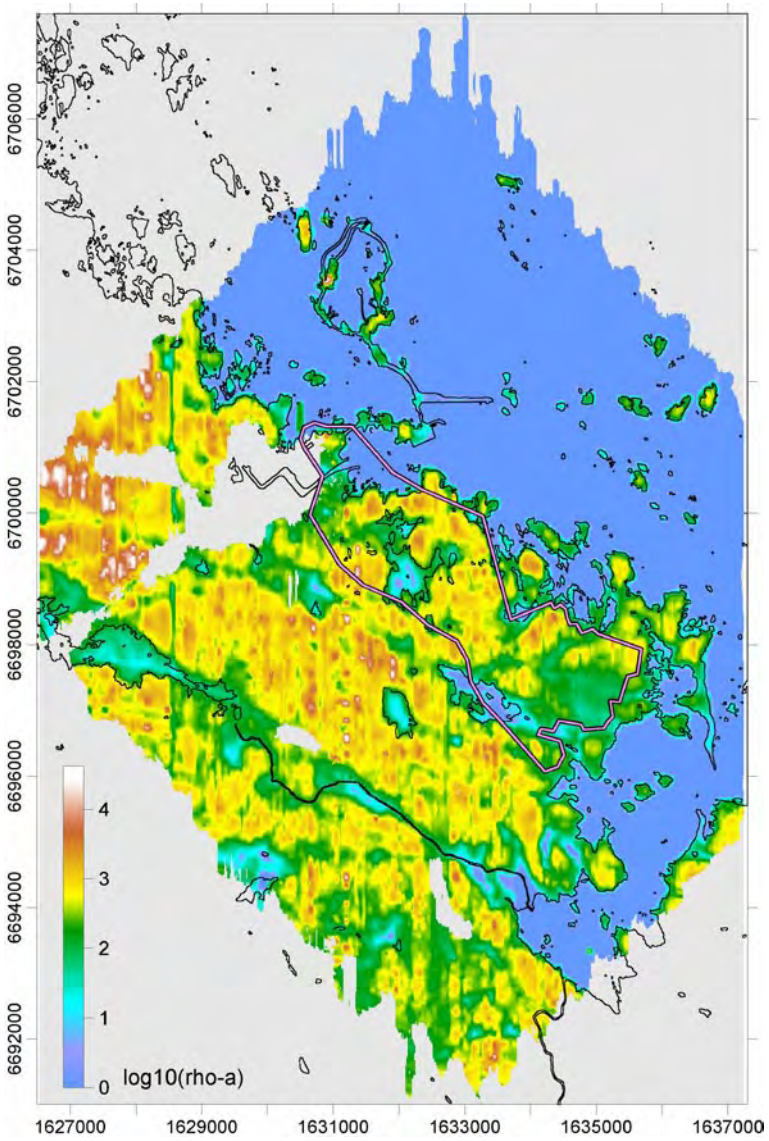


***Figure 4-9.*** *Map of apparent resistivity based on the quadrature component of the 34 kHz helicopter EM measurements, NS survey. The candidate area is marked with a black/pink line.*

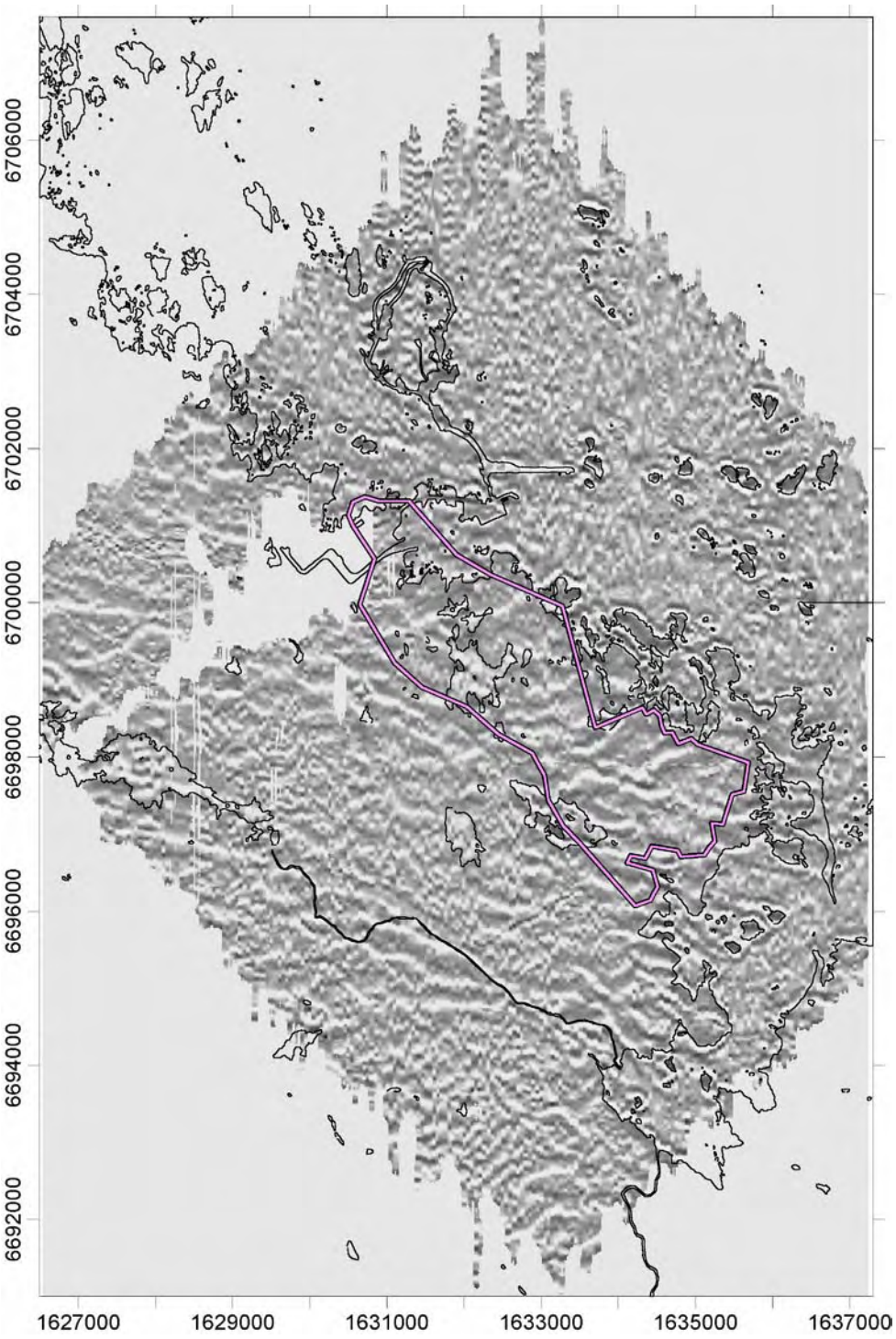


***Figure 4-10.*** *Map of AGC-filtered quadrature component data of the 34 kHz helicopter EM measurements, NS survey. The candidate area is marked with a black/pink line.*

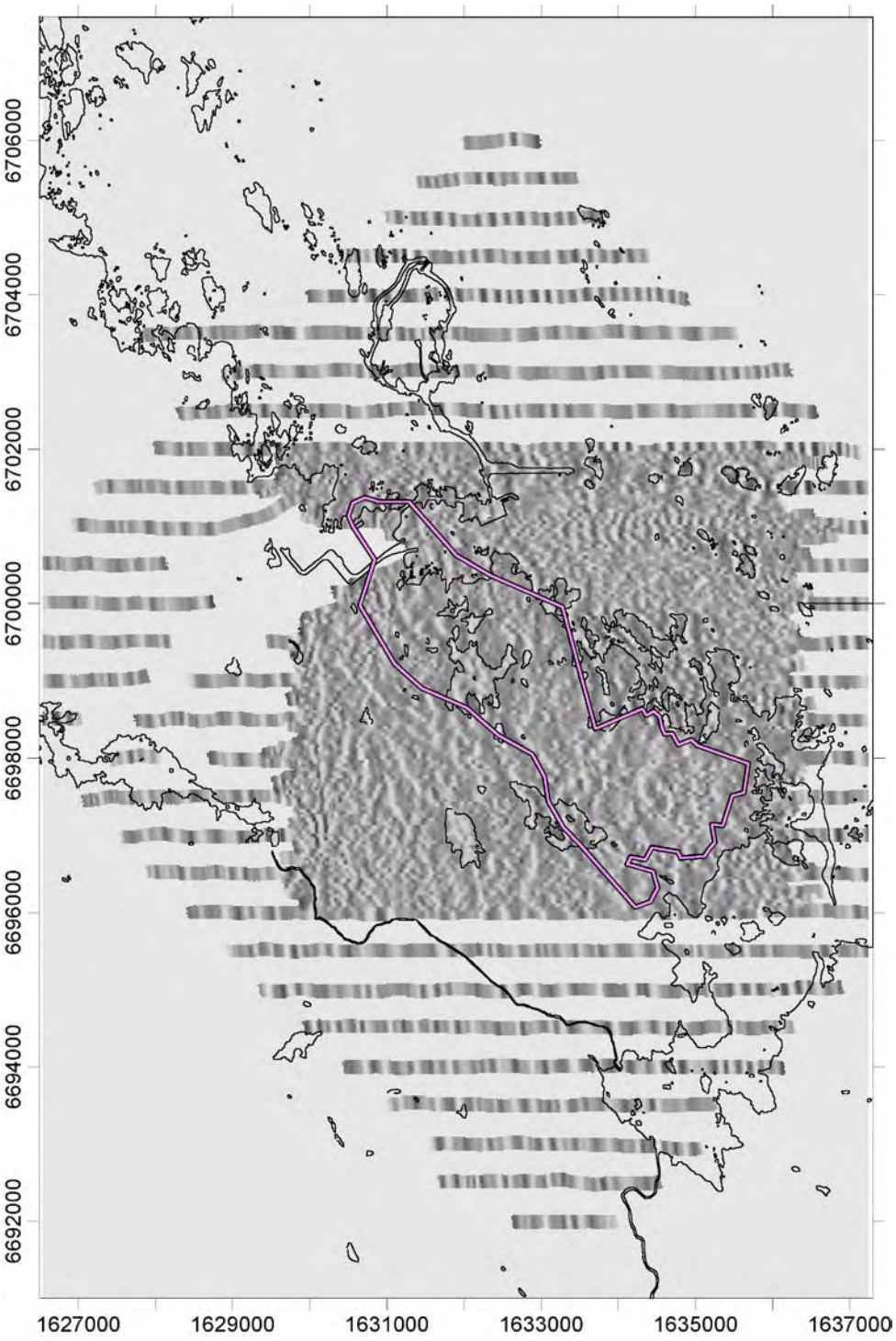


***Figure 4-11.*** *Map of AGC-filtered quadrature component data of the 34 kHz helicopter EM measurements, EW survey. The candidate area is marked with a black/pink line.*

### 4.3.2 Results

The interpretation was performed on screen with the help of GIS and image processing software where image layers could be turned on and off. Lineaments are seen as minima in apparent resistivity and maxima in the other image layers. Only those lineaments that could be seen in data from more than one measurement frequency were marked. Lineaments on land were mainly identified with the help of the quadrature components of the high and medium high frequencies, since fracture zones are expected to cause significant anomalies in these components only. However, EM fields of these frequencies are attenuated by water, so the lower frequencies were used to identify lineaments in water covered areas. Lineaments identified on land and water respectively, according to the procedure above, have been joined at the shoreline if they meet and have roughly the same direction. Lineaments that strike with an oblique angle relative the flight lines might be possible to identify both in the EW and the NS survey data. If such lineaments from the EW survey link with lineaments from the NS survey, they have been joined to one longer lineament. The work is thus to be regarded as a joint interpretation of several data layers. Based on their clarity and in how many components they could be identified, the lineaments were classified into the three groups: high, medium and low uncertainty.

The result of the lineament interpretation of EM data can be seen in Figures 4-12 to 4-15. With a few exceptions, the identified lineaments are shorter than 1 km. Most of the longer lineaments mainly have WNW-ESE strike direction.

In total, 411 electromagnetic, slingram lineaments have been defined. Based on the attached attribute table, Table 4-5, some general statistical results is presented, see Table 4-4. The interpretation results are stored in GIS-format and each unit has an attribute table attached, see also Table 4-5.

#### *Uncertainties*

It should be kept in mind that lineaments with a strike direction roughly N-S only have been possible to identify in the area covered by the EW survey lines (Figure 4-1). Also, due to poor data quality and increased flight altitude it has not been possible to identify any lineaments close to the major power lines in the western part of the survey area. The area close to the power plant is not covered by any survey lines.

EM lineaments have been marked without any discrimination due to the possible source unless it is obvious that it has been caused by some cultural source as e.g. power lines. EM lineaments might be caused by structures in the bedrock as well as in the overburden or as a combination of both. Also, it cannot be ruled out that some lineaments can be the effect of unknown cultural sources.

Only narrow lineaments corresponding to secondary field maxima and no areas with anomalous resistivity or borders to such areas have been marked. Some areas exist where the apparent resistivity is low e.g. around Storskäret and at Bruksdammarna. The low apparent resistivities in these areas are most likely the effect of fairly thick and/or conducting overburden. At this point it is very difficult to say anything about the resistivity of the bedrock in these areas. Careful levelling and inversion of the data into a two-layer model will probably sort out to what extent the low apparent resistivities are due to overburden and to what extent they are due to bedrock effects.

Almost all of the lineaments in the sea have been classified as “high uncertainty”. The reason for this is that, due to EM field attenuation by sea water, it has only been possible to use the real component of the 880 Hz data. It is therefore, at this stage, difficult to discriminate anomalies caused by bedrock structures from edge effects at shorelines or under-water terrain structures.

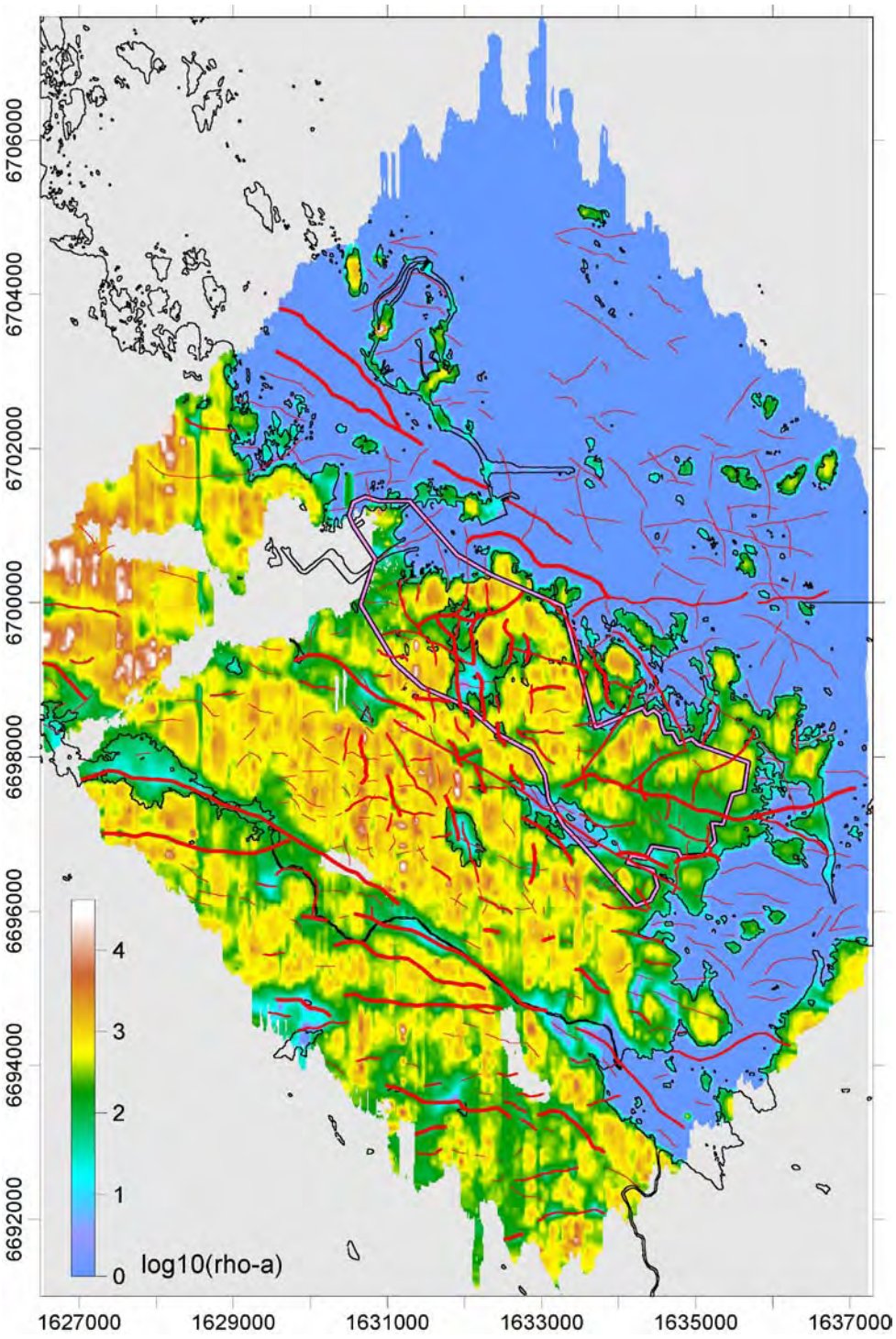


***Figure 4-12.*** *Map of apparent resistivity based on the quadrature component of the 34 kHz helicopter EM measurements, NS survey. The candidate area is marked with a black/pink line. Interpreted lineaments are shown as red overlays. Thick lines: low uncertainty, medium thick lines: medium uncertainty, thin lines: high uncertainty.*

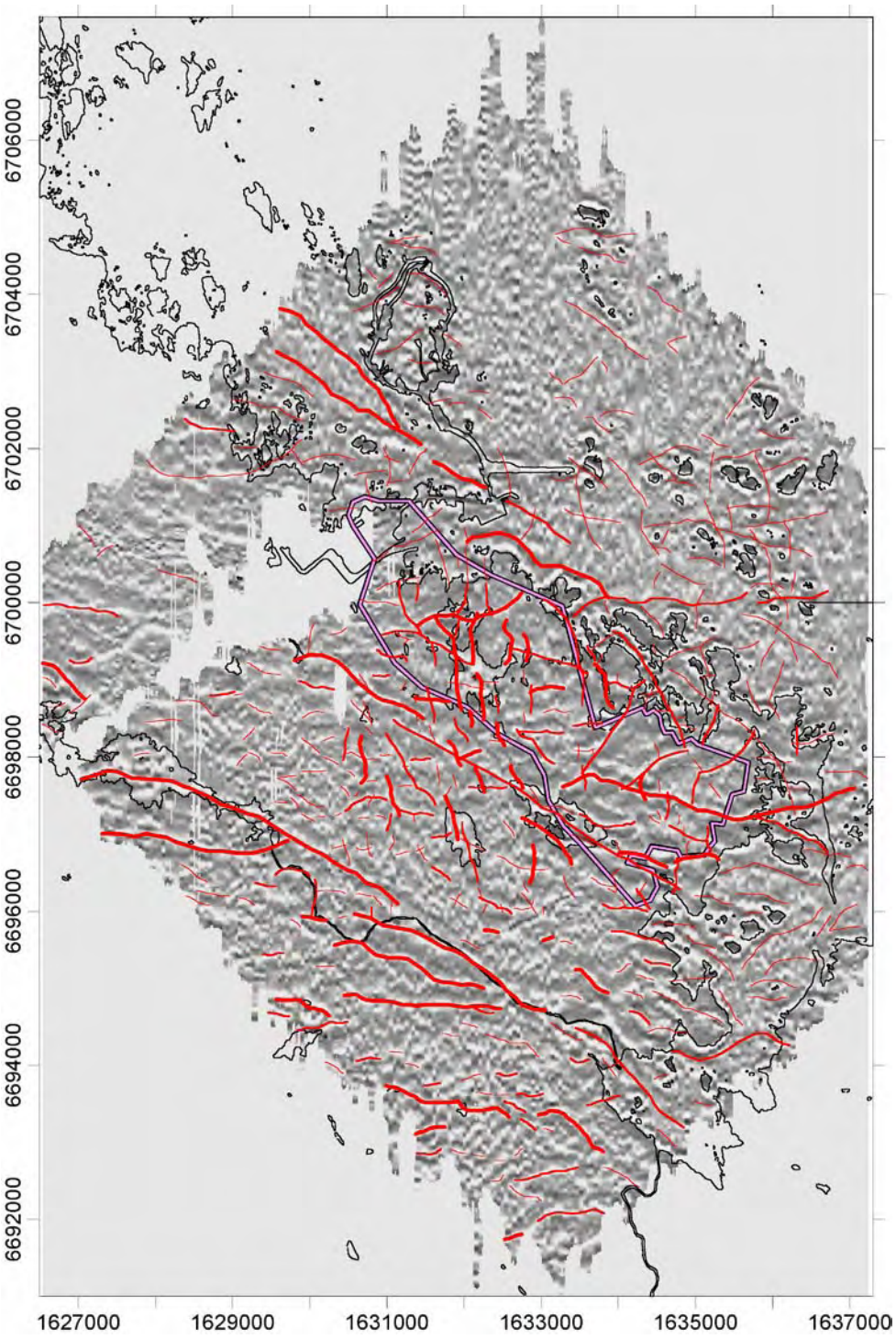


***Figure 4-13.*** *Map of AGC-filtered quadrature component data of the 34 kHz helicopter EM measurements, NS survey. The candidate area is marked with a black/pink line. Interpreted lineaments are shown as red overlays. Thick lines: low uncertainty, medium thick lines: medium uncertainty, thin lines: high uncertainty.*

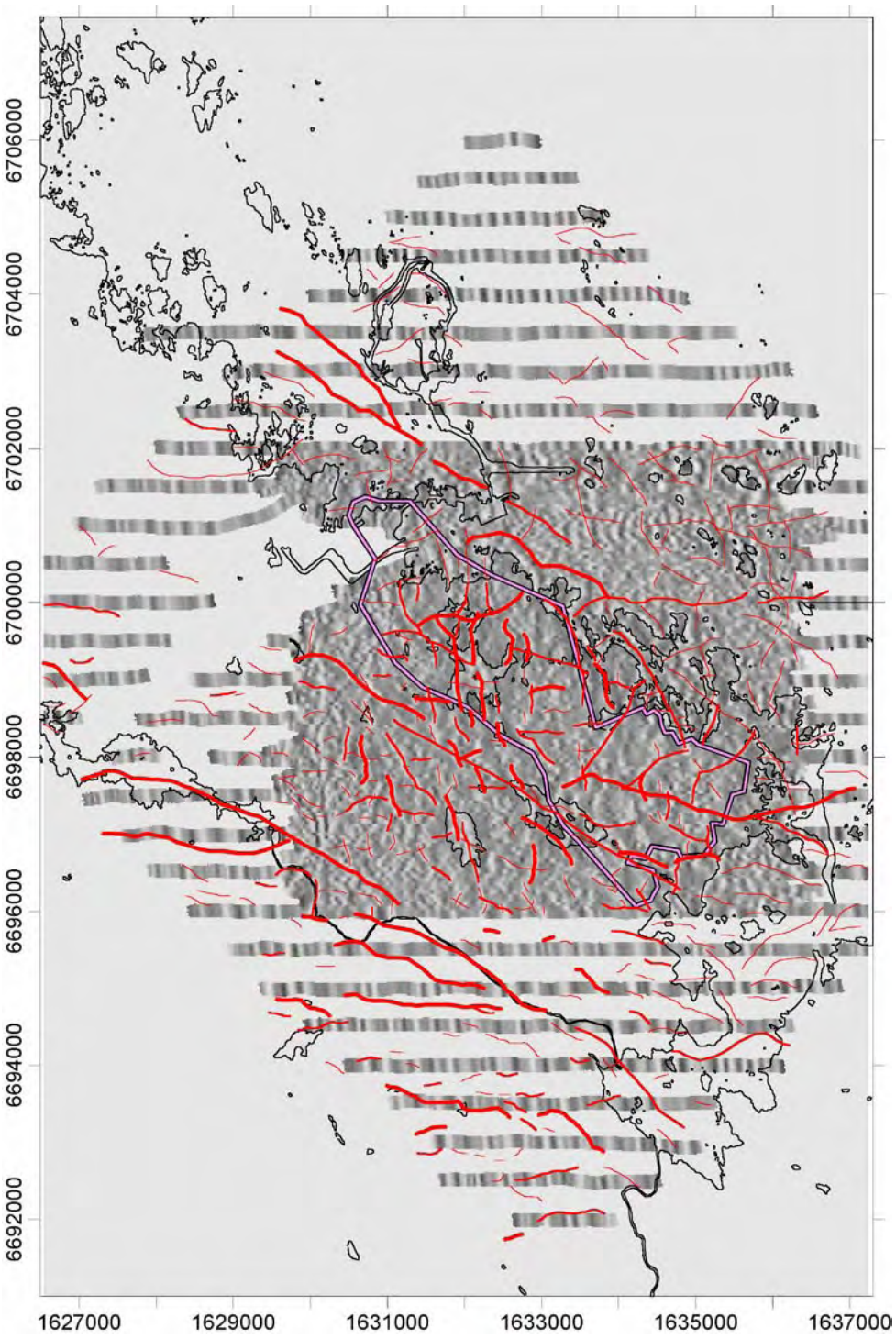


***Figure 4-14.*** *Map of AGC-filtered quadrature component data of the 34 kHz helicopter EM measurements, EW survey. The candidate area is marked with a black/pink line. Interpreted lineaments are shown as red overlays. Thick lines: low uncertainty, medium thick lines: medium uncertainty, thin lines: high uncertainty.*

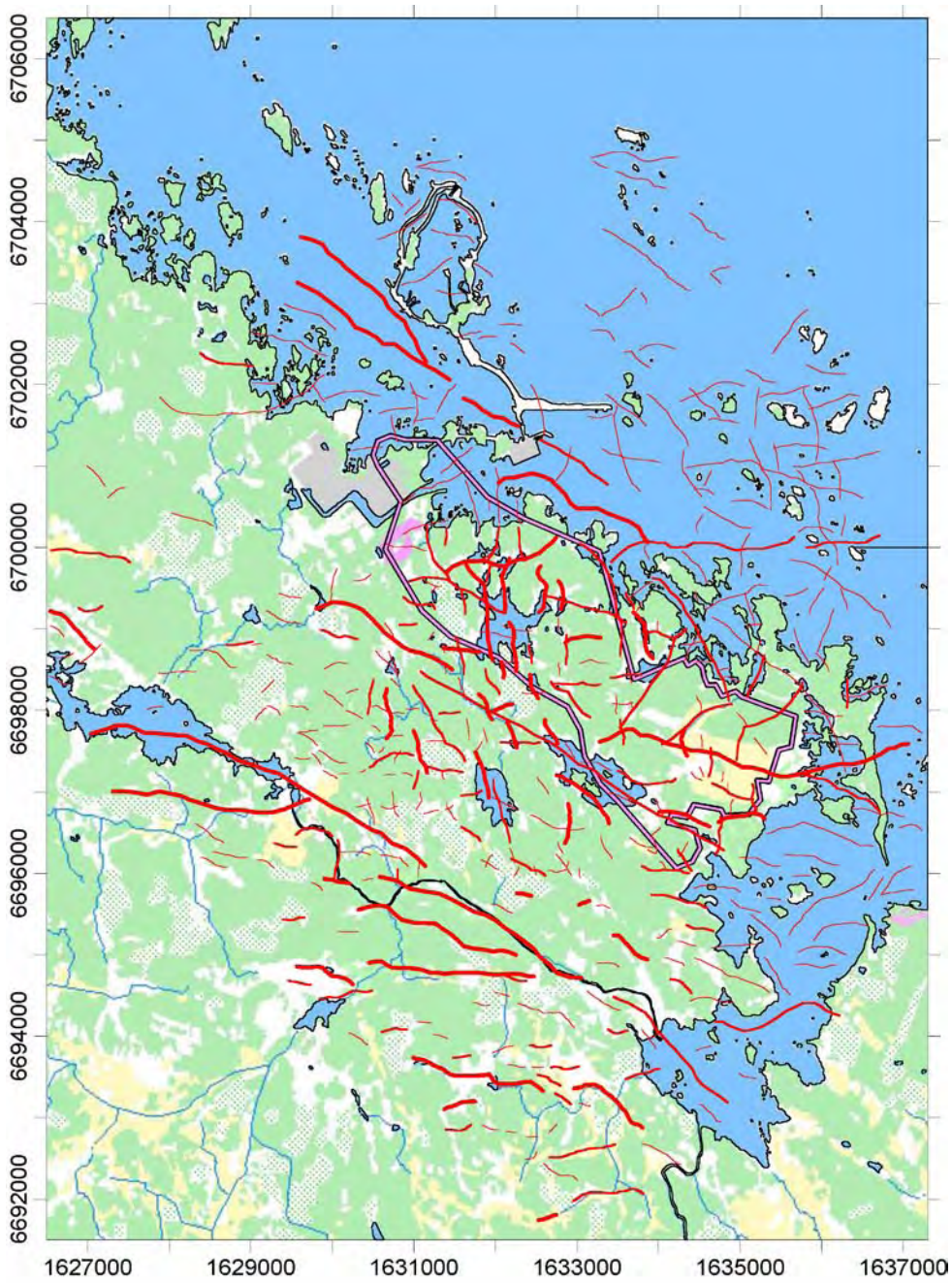


***Figure 4-15.*** *Map showing lineaments interpreted from helicopter EM data. The candidate area is marked with a black/pink line. Interpreted lineaments are shown as red overlays. Thick lines: low uncertainty, medium thick lines: medium uncertainty, thin lines: high uncertainty.*

**Table 4-4. Compilations of some attribute information for electromagnetic lineaments. Figures show number of occurrences.**

| Character | Low uncertainty | Medium uncertainty | High uncertainty | Total number |
|---|---|---|---|---|
| Maxima | 45 | 80 | 286 | 411 |

**Table 4-5. Attribute table for the electromagnetic lineaments.**

| Field name | Name | Description | Attribute used to describe EM lineaments |
|---|---|---|---|
| Id_t | Identity | Identity of the coordinated lineament | Not assigned in this work |
| Origin_t | Origin | Major type of basic data | Electromagnetic |
| Class_t | Classification | Classification of the coordinated lineament | Not assigned in this work |
| Method_t | Method | The type of data in which the observation is identified | Helicopter-EM, NS/EW-survey |
| Char_t | Character | Character of the observation | Maxima |
| Uncert_t | Uncertainty | Gradation of identification, in terms of uncertainty | Low/Medium/High |
| Comment_t | Comment | Specific comments to the observation | |
| Process_t | Processing | Data processing performed | Removal of level shifts F1&F5, PC-filter, AGC, gridding, image analysis, GIS |
| Date_t | date | Point of time for interpretation | 20030425 |
| Scale_t | Scale | Scale of interpretation | 10000 |
| Platform_t | Platform | Measuring platform for the basic data | Airborne geophysics, helicopter bird at 30m altitude |
| Width_t | Width | Width on average | Not assigned in this work |
| Precis_t | Precision | Spatial uncertainty of position | 30–50m |
| Sign_t | Signature | Work performed by | ht (Hans Thunehed), GeoVista AB |

## 4.4 VLF

### 4.4.1 Data processing

Basic data processing of VLF data was performed by the contractor /6/ and no further processing has been performed.

### 4.4.2 Results

The interpretation was performed on screen with the help of GIS and image processing software where image layers could be turned on and off. Only total field anomaly maps were used. Lineaments caused by conductors are seen as maxima in these image layers. Since measurements were made on fields from two VLF-transmitters and in two survey directions a total of four image layers were used. Based on their clarity and in how many components they could be identified, the lineaments were classified into the three groups: high, medium and low uncertainty.

The result of the lineament interpretation of VLF data can be seen in Figures 4-16 to 4-18.

In total, 94 VLF lineaments have been defined. Based on the attached attribute table, Table 4-7, some general statistical results are presented, see Table 4-6. The interpretation results are stored in GIS-format and each unit has an attribute table attached, see also Table 4-7.

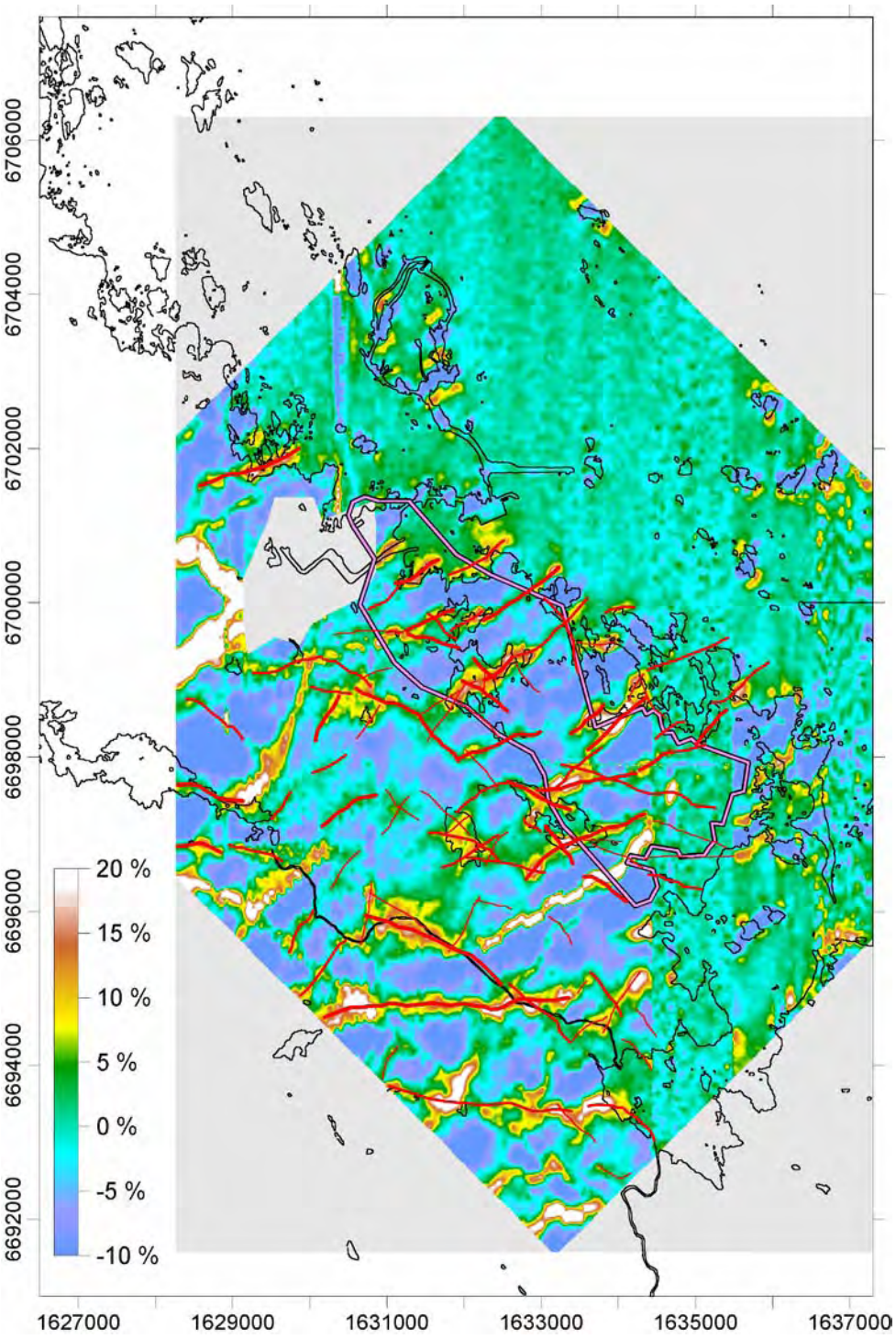


***Figure 4-16.*** *Map of total field VLF anomaly, in-line sensor, NS survey. The candidate area is marked with a black/pink line. Interpreted lineaments are shown as red overlays. Thick lines: low uncertainty, medium thick lines: medium uncertainty, thin lines: high uncertainty. The area around easting 1635000 is not measured with the default VLF transmitter.*

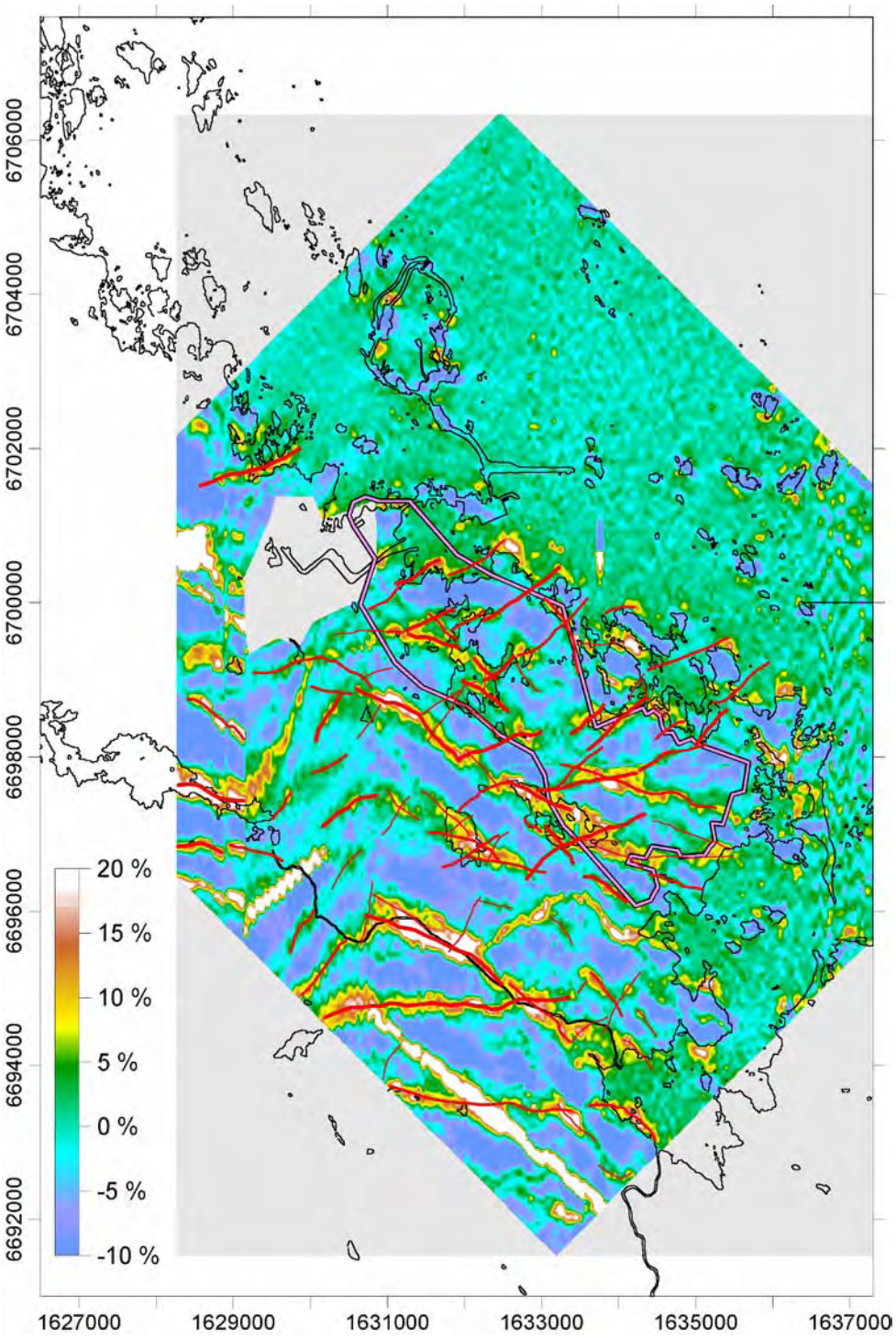


***Figure 4-17.*** *Map of total field VLF anomaly, orthogonal sensor, NS survey. The candidate area is marked with a black/pink line. Interpreted lineaments are shown as red overlays. Thick lines: low uncertainty, medium thick lines: medium uncertainty, thin lines: high uncertainty. The area around easting 1630000 south of northing 6700000 is not measured with the default VLF-transmitter.*

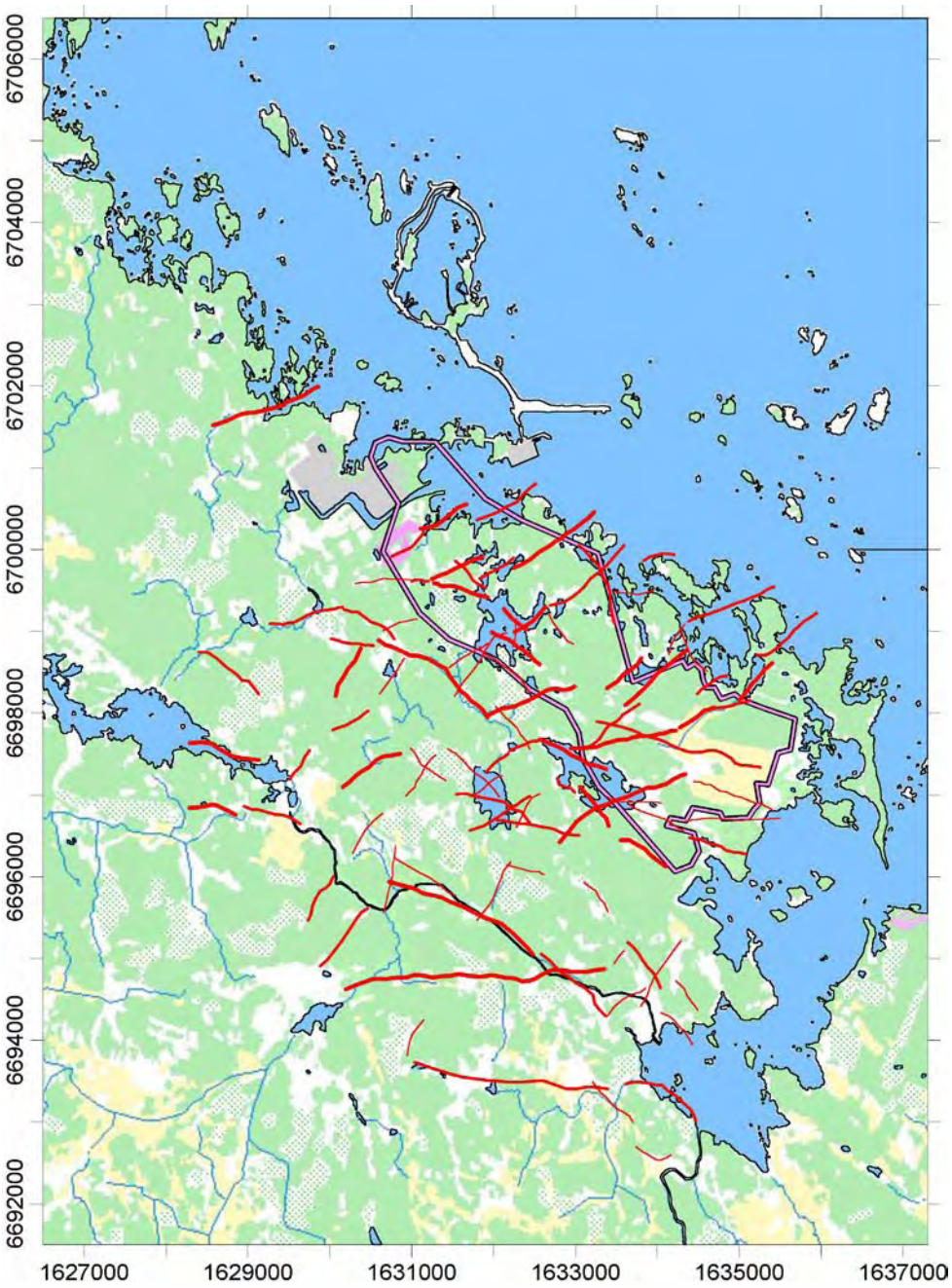


***Figure 4-18.*** *Map showing lineaments interpreted from helicopter VLF data. The candidate area is marked with a black/pink line. Interpreted lineaments are shown as red overlays. Thick lines: low uncertainty, medium thick lines: medium uncertainty, thin lines: high uncertainty.*

**Table 4-6. Compilations of some attribute information for VLF lineaments. Figures show number of occurrences.**

| Character | Low uncertainty | Medium uncertainty | High uncertainty | Total number |
|---|---|---|---|---|
| Maxima | 25 | 34 | 35 | 94 |

**Table 4-7. Attribute table for the VLF lineaments.**

| Field name | Name | Description | Attribute used to describe VLF lineaments |
|---|---|---|---|
| Id_t | Identity | Identity of the coordinated lineament | Not assigned in this work |
| Origin_t | Origin | Major type of basic data | VLF |
| Class_t | Classification | Classification of the coordinated lineament | Not assigned in this work |
| Method_t | Method | The type of data in which the observation is identified | Inline/Ortho and NS/EW-survey |
| Char_t | Character | Character of the observation | Maxima |
| Uncert_t | Uncertainty | Gradation of identification, in terms of uncertainty | Low/Medium/High |
| Comment_t | Comment | Specific comments to the observation | |
| Process_t | Processing | Data processing performed | Lag correction, levelling of lines, gridding, image analysis, GIS |
| Date_t | date | Point of time for interpretation | 20030425 |
| Scale_t | Scale | Scale of interpretation | 10000 |
| Platform_t | Platform | Measuring platform for the basic data | Airborne geophysics, Sensor below heli copter, two frequency |
| Width_t | Width | Width on average | Not assigned in this work |
| Precis_t | Precision | Spatial uncertainty of position | 50m |
| Sign_t | Signature | Work performed by | ht (Hans Thunehed), GeoVista AB4.5 |

#### *Uncertainties*

VLF measurements are direction sensitive by nature. Two transmitters were used to enable the identification of lineaments in different directions. However, the two VLF transmitters that were used by default do not have orthogonal primary fields in the Forsmark area. They had maximum sensitivity for structures striking WSW-ENE and ESE-WNW respectively. NS striking lineaments might therefore be under-represented in the interpretation. A different transmitter was used if one of the default transmitters was off during a flight, since delays of the survey completion had to be avoided. This resulted in problems in the interpretation since the transmitters that replaced the default ones had different directions of the primary field. The power lines produce strong anomalies in the VLF measurements. These anomalies will, in general, mask the appearance of anomalies caused by geological structures.

The westernmost part of the survey area is not covered by VLF data due to an instrumental failure during the survey.

## 4.5 Gamma ray spectrometry

### 4.5.1 Data processing

The apparent thorium, potassium and uranium concentrations at the ground surface as well as the total exposure rate have been interpolated to 10 × 10 m grids by means of a median interpolation routine (Surfer 8). Both survey directions have been interpolated together and the search radius was 87.5 m. The result is presented as a colour composite, with R,G,B=Th,K,U in Figure 4-19.

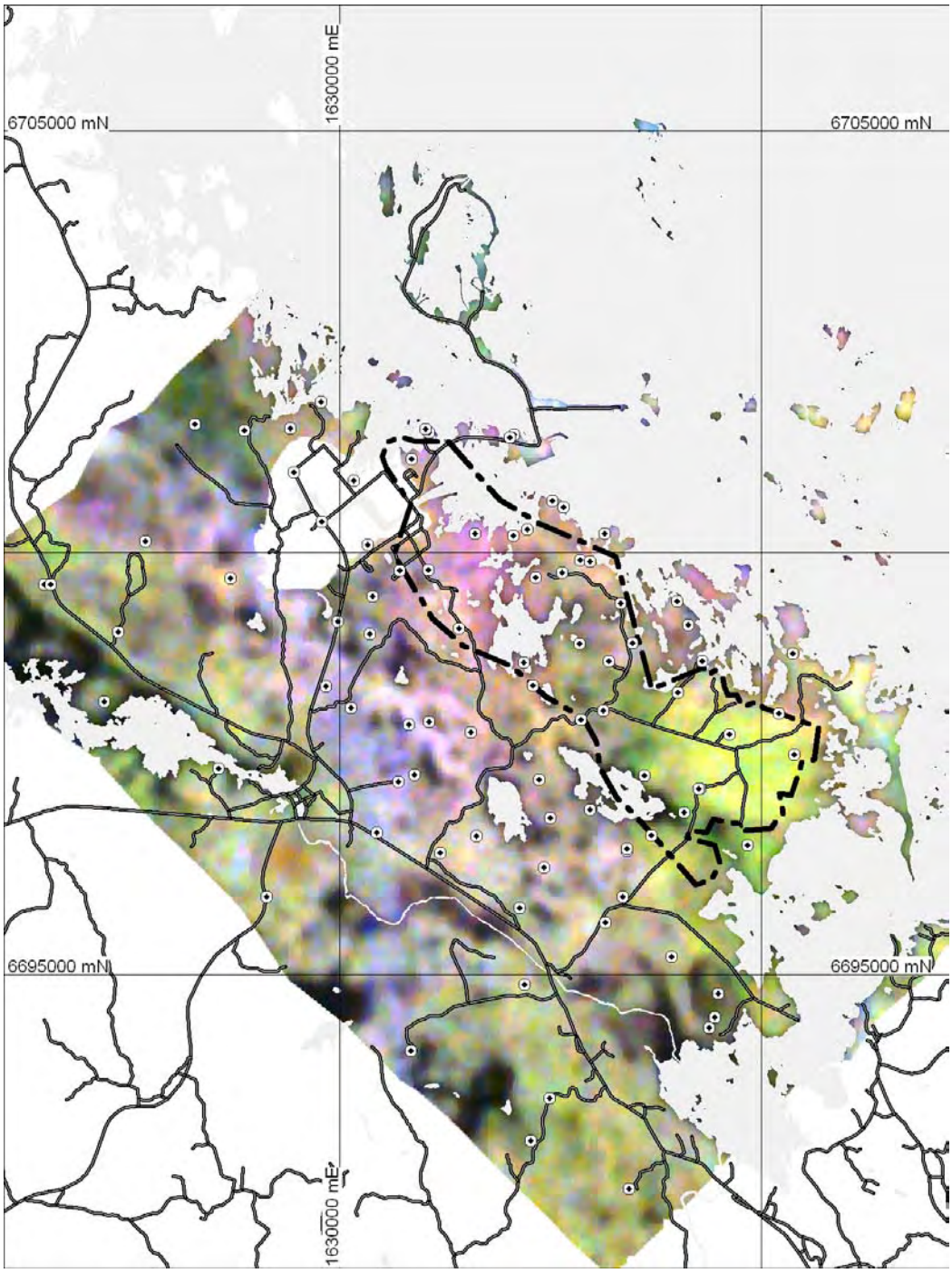


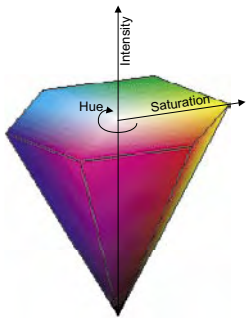


| *Colour* | *Element* | *Low intensity, dark colours* | *High intensity, bright colours* |
|---|---|---|---|
| *Red* | *Thorium* | *–0.5 ppm* | *11.5 ppm* |
| *Green* | *Potassium* | *–0.2%* | *2.3%* |
| *Blue* | *Uranium* | *–0.1 ppm* | *3.9 ppm* |

*Hue and saturation describes the relative distribution of the elements. The total colour intensity indicates the total gamma radiation.*

***Figure 4-19.*** *Airborne gamma-ray spectrometry presented as a RGB, colour composite. Forsmark candidate area outlined with black, dot-dashed line. Gamma-ray spectrometry measurements on out-crops with black-white dots.*

After interpolation, the data was visually inspected for typical groups of element and total exposure combinations. By means of image analysis (Geomatica – ™ PCI), training areas were selected covering the most evident anomaly patterns. Some areas were selected to cover areas with low gamma radiation, like the sea, lakes and marshes. In addition some well exposed farmlands with different characteristics were also selected. For characteristics with probable correlation to moraine and/or bedrock, the training areas were selected to areas with high outcrop exposure and upland topography.

After an iterative process, in which classes with very similar characteristics were joined together, finally 12 classes were established. The characteristics of the training areas selected, provided the foundation for a maximum likelihood classification, using the equation for Mahalanobis minimum distance /8, 9/. Location of the training areas is presented in Figure 4-20 and the result of the classification is presented in Figure 4-21. Areas with a low probability (< 50%) were not classified. These areas are also outlined in Figure 4-21 (Section 4.5.2).

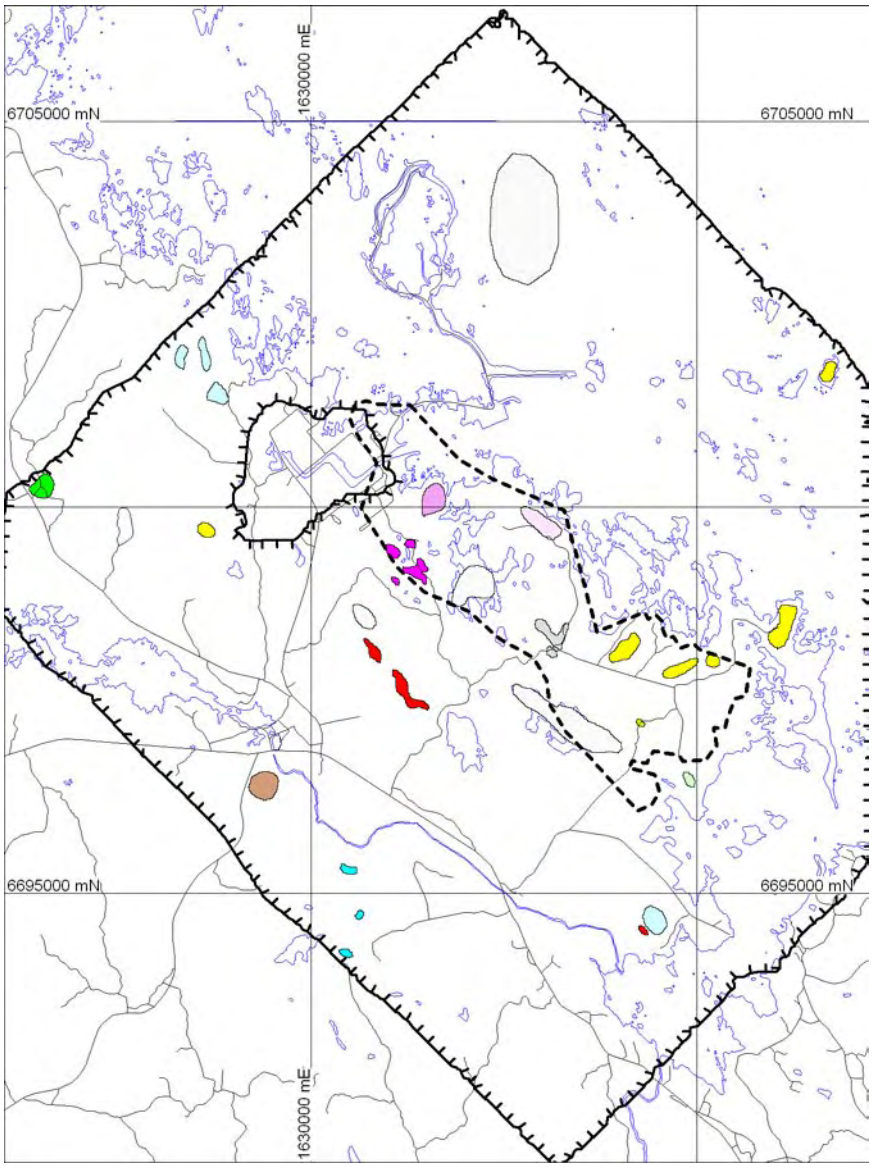


***Figure 4-20.*** *Training areas for the maximum likelihood classification of the airborne gamma-ray spectrometry. Colours correspond to the legend in Figure 4-21.*

### 4.5.2 Results

The final results from the maximum likelihood classification are compiled in Table 4-8.

The airborne gamma-ray spectrometry gives data for the upper part of the ground surface and to understand the classification pattern, information about the quaternary cover is important. Only in areas with very good bedrock exposure the data give direct information on rock radiometric parameters. Hence, gamma-ray spectrometry measurements on outcrops should be used in the interpretation of the radiometric pattern. Below follows some comments to the classification results:

The airborne gamma-ray spectrometry survey covered about 104 km², but only 101 km² was classified, since the area around the Forsmark power plant was excluded. The total area, with a low probability to belong to the assigned class, is 0.8 km² or < 1% of the classified area.

The sea, lakes and marshes, and other wetland give low gamma radiation. The corresponding class called "Water", covers 44.4 km², or 44% of the area.

The class "Low Th, K, U intensity", commonly also corresponds to wetland areas. However, in upland terrain and in well exposed areas, this group probably corresponds to mafic-ultramafic rock units. The class covers 13.8 km² or 14% of the area.

Background Th, K, U levels partly overlap with a class showing somewhat lower potassium values. The latter is recognized in conjunction with some farmlands. In total, these two classes cover 20.5 km² or 20% of the area.

A class, "K-dominant, medium intensity" mainly occurs along the Forsmarks bruk–Johannisfors valley. The cause of this pattern in not yet understood.

**Table 4-8. Compilation of results from the maximum likelihood classification of the airborne, gamma-ray spectrometry. The class name, "LegendText", corresponds to the names used in Figure 4-21.**

| Class No | LegendText | Ka (%) | U (ppm) | Th (ppm) | Natural exposure (microR/h) | K stdv (%) | U stdv (ppm) | Th stdv (ppm) | Natural exposure stdv (microR/h) | Count | Area (km2) |
|---|---|---|---|---|---|---|---|---|---|---|---|
| 1 | Water | 0,09 | 0,39 | 0,56 | 0,56 | 0,17 | 0,38 | 1,11 | 0,76 | 49 | 44,45 |
| 2 | Low Th,K,U intensity | 0,93 | 1,39 | 4,68 | 3,69 | 0,22 | 0,47 | 1,10 | 0,80 | 188 | 13,82 |
| 3 | K low, background Th,U levels | 1,20 | 2,01 | 7,62 | 5,32 | 0,16 | 0,43 | 0,97 | 0,56 | 371 | 5,76 |
| 4 | Background Th,K,U levels | 1,51 | 1,93 | 7,48 | 5,72 | 0,14 | 0,39 | 0,89 | 0,48 | 269 | 14,74 |
| 5 | Th,K-dominant, medium intensity | 1,81 | 1,85 | 8,25 | 6,29 | 0,12 | 0,52 | 0,98 | 0,36 | 263 | 1,77 |
| 6 | U-dominant, medium intensity | 1,51 | 3,07 | 7,63 | 6,37 | 0,21 | 0,44 | 1,14 | 0,80 | 262 | 4,69 |
| 7 | Th,U-dominant, K low, medium intensity | 1,31 | 2,92 | 9,50 | 6,62 | 0,15 | 0,41 | 1,10 | 0,58 | 103 | 1,31 |
| 8 | K-dominant, medium intensity | 1,85 | 2,25 | 8,79 | 6,82 | 0,10 | 0,35 | 0,67 | 0,27 | 204 | 3,55 |
| 9 | Th,U-dominant, medium intensity | 1,63 | 2,59 | 9,53 | 6,88 | 0,12 | 0,35 | 0,74 | 0,38 | 274 | 5,32 |
| 10 | Th,K-dominant, high intensity | 2,11 | 2,30 | 10,21 | 7,64 | 0,20 | 0,58 | 1,00 | 0,45 | 108 | 3,82 |
| 11 | Th,U-dominant, high intensity | 1,78 | 3,22 | 10,78 | 7,89 | 0,11 | 0,33 | 0,86 | 0,31 | 98 | 0,93 |
| 12 | High Th,K,U intensity | 1,87 | 3,83 | 10,41 | 8,30 | 0,15 | 0,52 | 1,11 | 0,62 | 93 | 0,85 |
| | Other areas | | | | | | | | | | |
| | Class probability <50% | | | | | | | | | 119 | 0,75 |
| | Classified area | | | | | | | | | 1 | 101,13 |
| | Forsmark power plant, not classified | | | | | | | | | 1 | 2,51 |

A distinct class is “U-dominant, medium intensity”, for which the geographical pattern indicates a south-north extension, east of the Forsmarks bruk, and continuing in the north-west direction, south of the Forsmark power plants. In part, this pattern corresponds to the airborne survey direction and hence, a levelling problem can be considered. This has to be examined in more detail during the geological mapping in 2003. This class covers 4.7 km² or 5% of the area.

Areas with high gamma-ray intensity are concentrated to an area between Eckarfjärden and Gällsboträsket and further to the northwest, south of the Forsmark power plants. In this area, pegmatite and pegmatitic granite are common and can probably explain this pattern /3/. This class covers an area of 0.8 km².

The classification pattern within the Forsmark candidate area is characterized by three, rather distinct patterns:

In the central part, from Bolundsfjärden to Fiskarfjärden and around drill site 2, background levels and/or low Th,K,U intensity are most common.

Around Storskäret, in the southeast part of the candidate area, thorium and potassium are clearly dominating and often show rather high intensities. This class corresponds not only to the well exposed farmland at Storskäret, but also to more upland terrain which, in part, is boulder rich and exposes fairly large outcrop areas. This indicates that the Th, K-pattern can be related, at least partly, to the bedrock and this also corresponds to the pattern obtained for pegmatitic granite in the gamma-ray spectrometry performed on outcrops /3/.

The area from Bolundfjärden and Norrskäret and further to the northwest shows a clear thorium and uranium dominance. Around drill site 1 and to the southwest, the intensities are also relatively high. Of special interest is that this area also is characterized by generally low potassium content.

The special features occurring within the candidate area can be important for the site investigation process and have to be studied in more detail during the bedrock mapping in 2003 and possibly also by gamma-ray spectrometry loggings in drill holes.

### *Uncertainties*

As mentioned earlier, the airborne gamma-ray spectrometry gives information on radiometric levels for the uppermost part of the ground surface. In areas with large outcrop exposure and uncomplicated bedrock geology the airborne data should correspond well to gamma-ray spectrometry data measured on the outcrops. However, such a comparison between the gamma-ray spectrometry measurements on outcrops /3/ and the airborne survey results give a rather poor correlation for all three elements.

A preliminary comparison of the apparent Th, K and U-levels between the 2002 NGU survey and the previous SGU surveys, indicate that the levels correspond rather well at 0-levels (water) and at background levels, 7 ppm Th, 1.5–2.0% K and 2 ppm U respectively. However, at least for higher values than background, the NGU data presents much lower levels than the corresponding SGU data. For the level 14 ppm Th at the SGU surveys, NGU reports 9–10 ppm. For 3% K, NGU reports 2.2–2.4% K and finally for 4 ppm U, NGU reports 2.0–2.5 ppm.

For further work with the airborne gamma spectrometry data, it is recommended to study the previous levelling and calibration of the NGU-data and evaluate if further processing is required to improve the quality. No such study has been performed during the airborne survey project /Sören Byström, SGU, oral communication/.

Should this study show that a recalibration is necessary, this will of course also have an influence on the levels reported in Table 4-8. However, the classification and the classified areas will probably only be affected to a minor extent.

These results will be further examined in the next stage, 2003–2004.

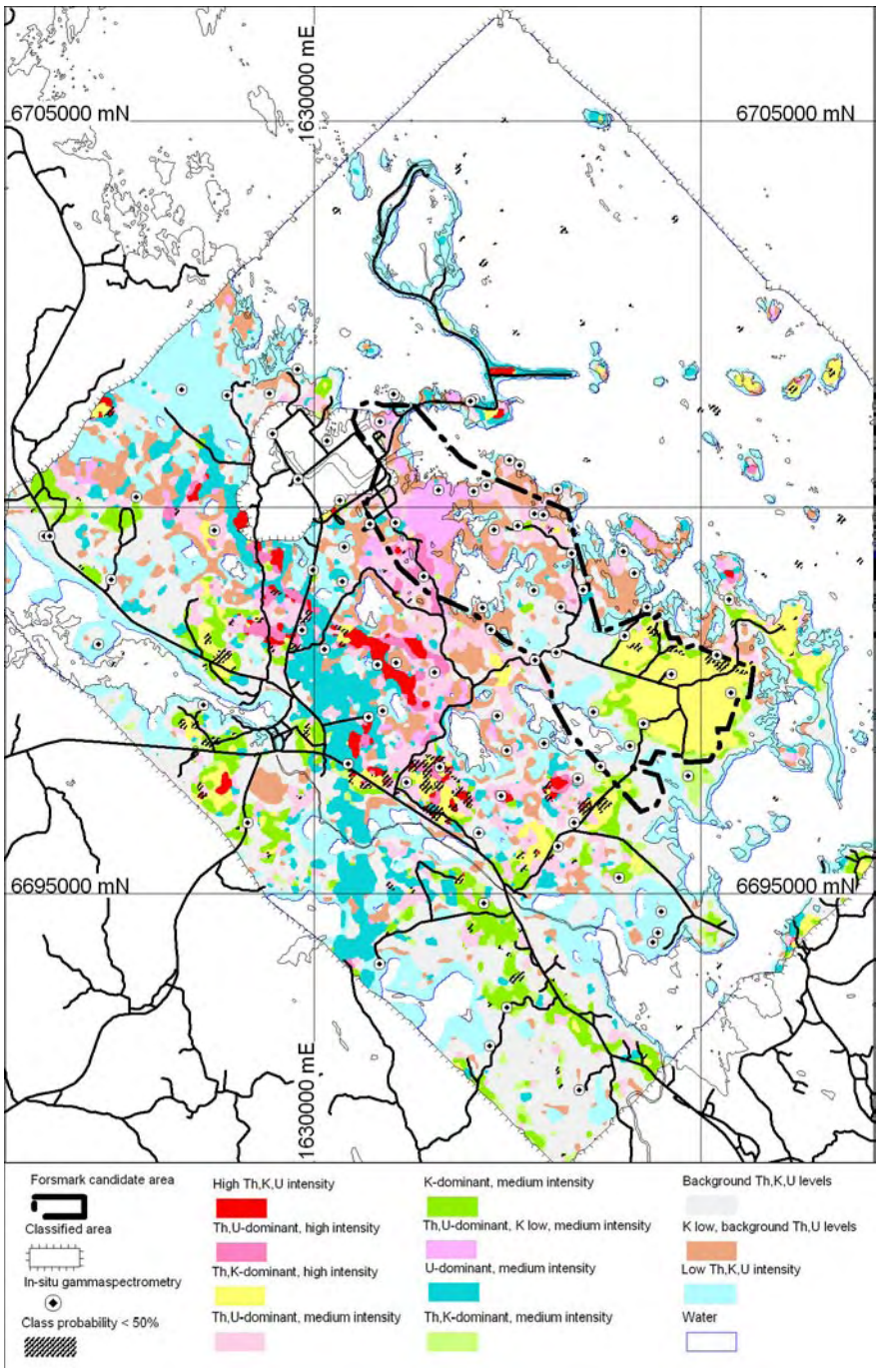


***Figure 4-21.*** *Airborne gamma-ray spectrometry, maximum likelihood classification.*

# 5 Coordination of airborne geophysical and topographical lineaments

Coordination of lineaments has been carried out according to procedures and methodologies described in “Geological site descriptive model. A strategy for the model development during site investigations” /1/. A coordinated lineament is characterized by the methods identifying the lineament and the length limited to each unique method composition. This means that a lineament is split when and if a new method identifies the lineament. This process is adopted even though there is a high degree of confidence that the lineament is continuous. The coordinated lineaments form a basis for the subsequent linking of the lineament segments together into a linked lineament, see Chapter 6.

The area used for the coordination of lineaments is concentrated to the mainland area since no topographic data was accessible in the sea area. The airborne EM and VLF data also give limited possibilities to delineate structures in the sea area, see Chapter 4.3.2. In the sea area the “coordinated” lineaments are therefore represented by a copy of the magnetic lineaments and a boundary that defines the area for which the coordination of lineaments has been performed, see Figure 5-4.

Further processing of the airborne EM data (inversion) as well as access to marine geological and bathymetrical data will provide better possibilities for future lineament interpretations and co-ordination of lineaments in the sea area.

## 5.1 Input data

Input to the coordinated lineament interpretation has been the following method specific lineament data sets:

- Topographic lineaments (see Figure 5-2).
- Magnetic lineaments (see Figure 4-5).
- EM lineaments (see Figure 4-15).
- VLF lineaments (see Figure 4-18).

In addition to these lineament GIS-layers, a number of processed images, covering the different methods, have also formed the basic input data.

No lineament feature was identified in the airborne gamma-ray spectrometry data.

The previous topographic lineament interpretation is further described in Chapter 5.1.1. It can be noted that, except for the topographic depressions that were previously outlined, also the industrial area around the Forsmark power plants is very flat due to extensive landfill, which gives rise to areas with very little or no topographic relief. These areas, together with the disturbed area in the helicopter-borne geophysical data, defines areas where the possibilities to delineate lineaments are limited.

### 5.1.1 Topographical data and interpretation

Topographical lineaments have previously been interpreted /10/. The work was carried out according to procedures and methodology described in “Metodbeskrivning för lineamentstolkning baserad på topografiska data” (SKB MD 120.001, v 1.0). The results from this work, in the form of lineaments and topographic images, have been included in the lineament coordination as GIS-layers. Figure 5-1 shows an example of an image processing of the elevation data to enhance narrow features. The resulting topographic lineaments from the interpretation are presented in Figure 5-2.

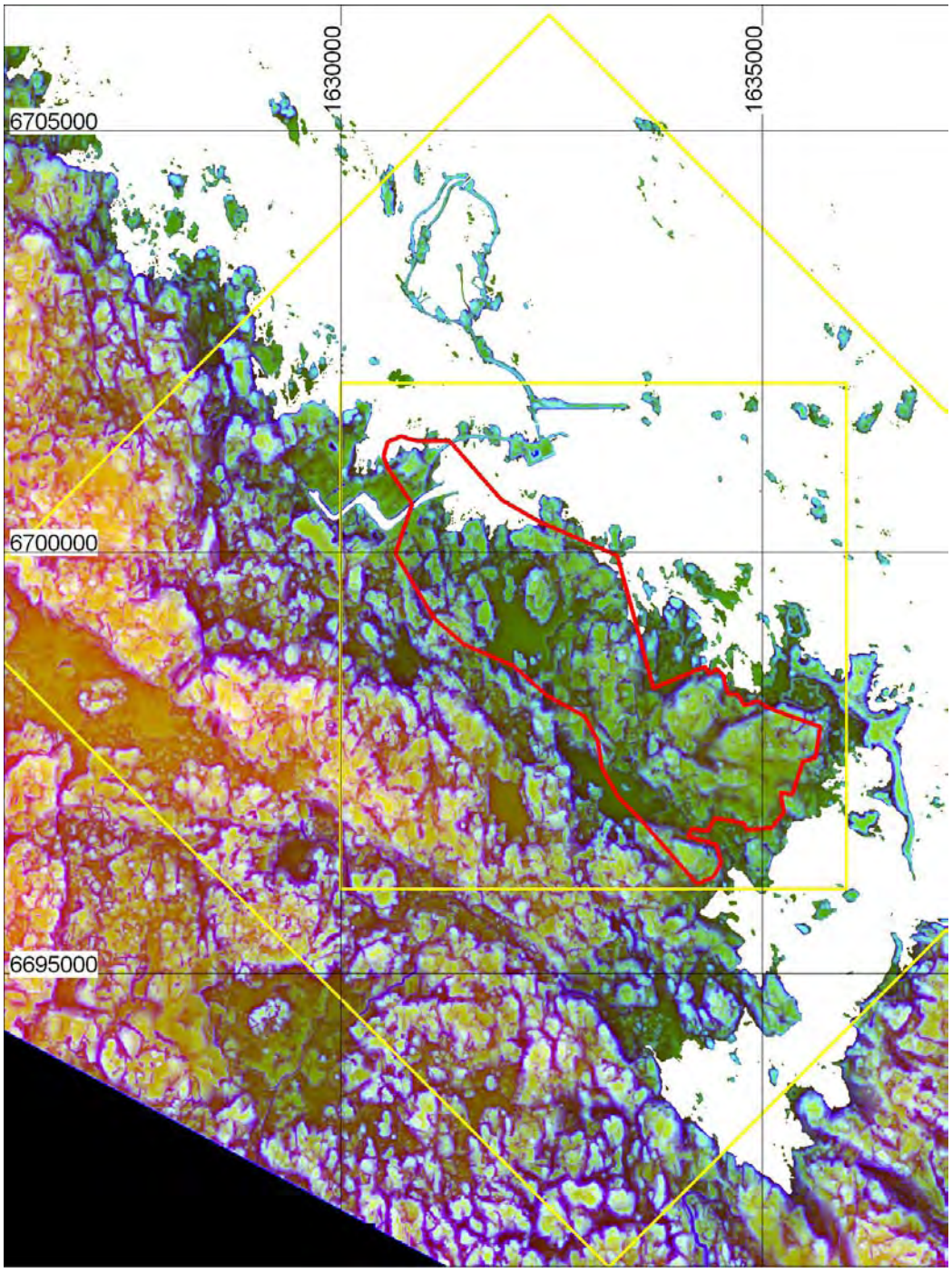


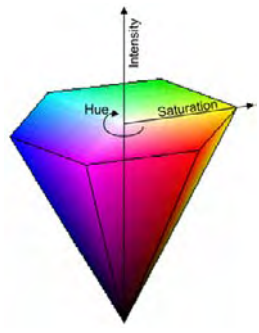


| *Colour* | *Element* |
|---|---|
| *Red* | *Elevation* |
| *Green* | *Elevation, edge sharpening* |
| *Blue* | *Elevation, slope* |

*Hue and saturation describes the relative distribution of the variables. Dark and bright colours indicate low and high values, respectively.*

***Figure 5-1.*** *Topographic data from the previous interpretation of topographic lineaments 2002 /8/, presented as a RGB, colour composite. Forsmark candidate area is outlined with a red line. Yellow markers outline the airborne geophysical survey areas.*

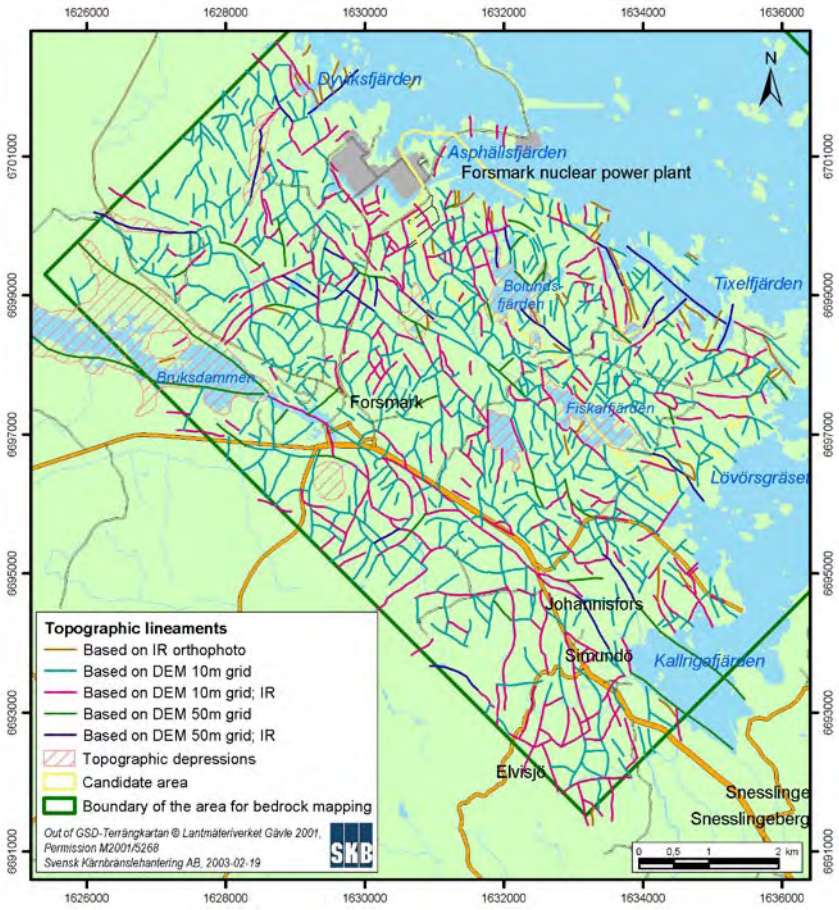


***Figure 5-2.*** *Topographic lineaments as presented in previous interpretation of topographic lineaments 2002, /8 (Figure 5-1)/.*

## 5.2 Lineament coordination

The interpretation has been carried out by visual characterization, using image analysis (Geomatica – ™ PCI) and GIS-techniques (Mapinfo – ™ Mapinfo). The coordination of lineaments on the mainland was performed according a specific methodology:

- All basic, method specific lineaments have been visualized together, with or without basic method background images.
- The method specific lineament that is judged to give the best spatial precision, or appear with the best clarity, is selected to represent the location of the coordinated lineament.
- Nearby, method specific lineaments based on other methods are then judged to either represent the same coordinated lineament or, alternatively, another coordinated lineament.
- The clarity of each method that delineates the coordinated lineament also defines a method ranking, i.e. magn, topo, EM, VLF. This ranking is noted in the field “Method_t”, in the adherent attribute table, see Table 5-2.
- When the lineament is no longer identified in a method, it is split, and a new coordinated lineament is defined with a new method ranking. The same is valid if a new basic method identifies the coordinated lineament.

- In difficult settlements, different basic method images are studied, to come to a conclusion. In some cases a method specific lineament has been considered as false and rejected. In some cases a lineament has also been extended or modified in position.
- The length of each coordinated lineament has been calculated. However, since a coordinated lineament is strictly divided according to the characteristic methods, the length measure is only used as a basis for the subsequent formation of a linked lineament, see Chapter 6.
- Also the direction of each coordinated lineament has been calculated.
- At sea, the lineaments are represented by a copy of the interpretation of magnetic lineaments and hence, the above methodology is not applicable. However, the lineaments are split at the divider to the mainland. The divider between the two data sets is outlined by a boundary; “sea_lineament_boundary”

Figure 5-3 shows an example of the lineament coordination procedure.

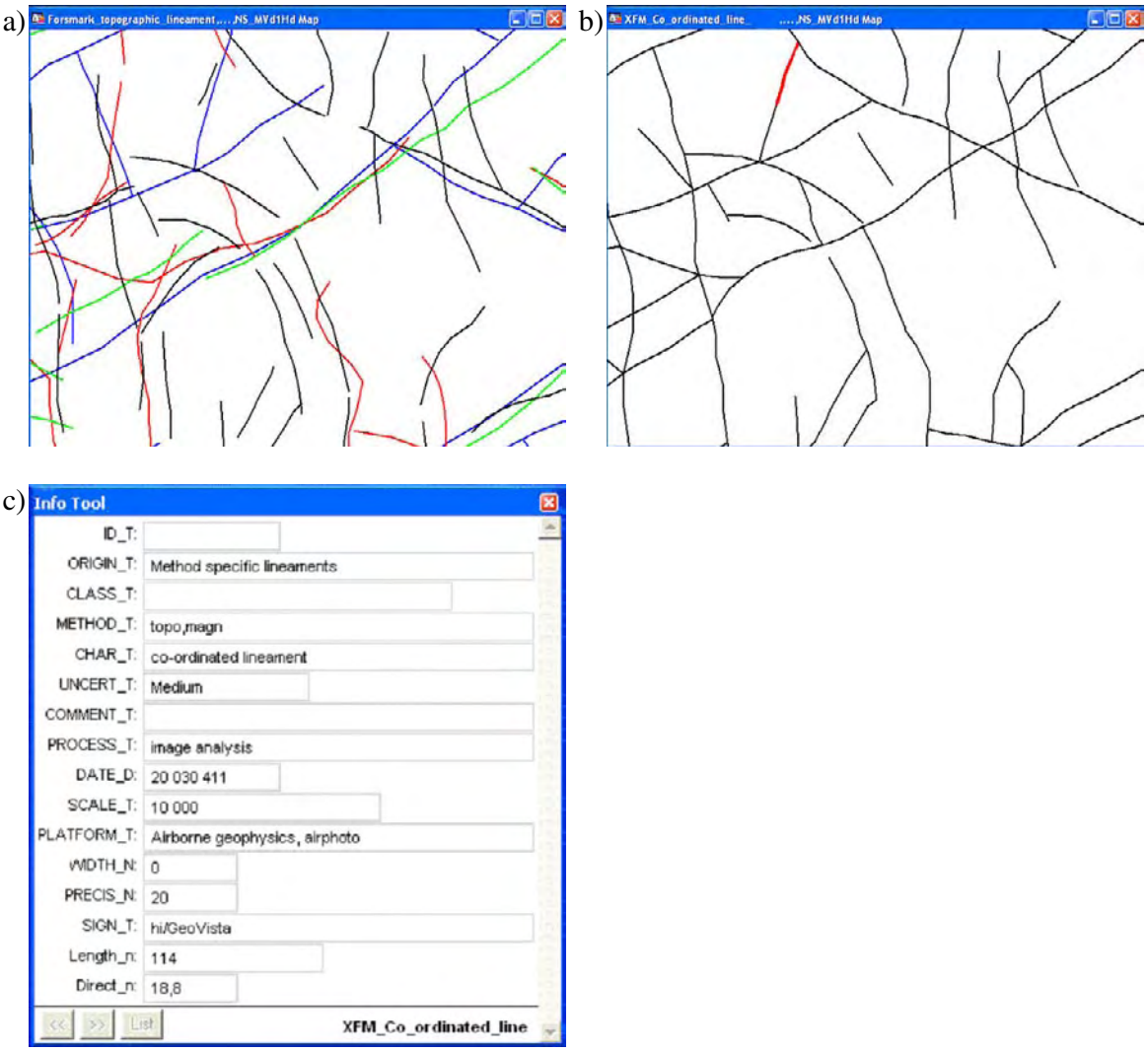


***Figure 5-3.*** *An example of lineament coordination. a) Method specific lineaments; magnetic, EM, VLF and topographical lineaments in blue, red, green and black respectively. b) The same area after lineament coordination. c) The attribute table for the red lineament marked in b).*

## 5.3 Results

Figure 5-4 shows the result of the lineament coordination. A complete coordination of lineaments has been performed on the mainland, while in the sea area, the lineaments are represented by a copy of the magnetic lineament interpretation. The divider between the two data sets is outlined by a boundary; “sea_lineament_boundary”.

In total, 1371 coordinated lineaments have been defined. Based on the attached attribute table, Table 5-2, some general statistical results are presented, see Table 5-1.

A total of 82 “coordinated”, magnetic lineaments are defined in the sea area, see also Table 5-1.

The interpretation results are stored in GIS-format and each unit has an attribute table attached, see also Table 5-2.

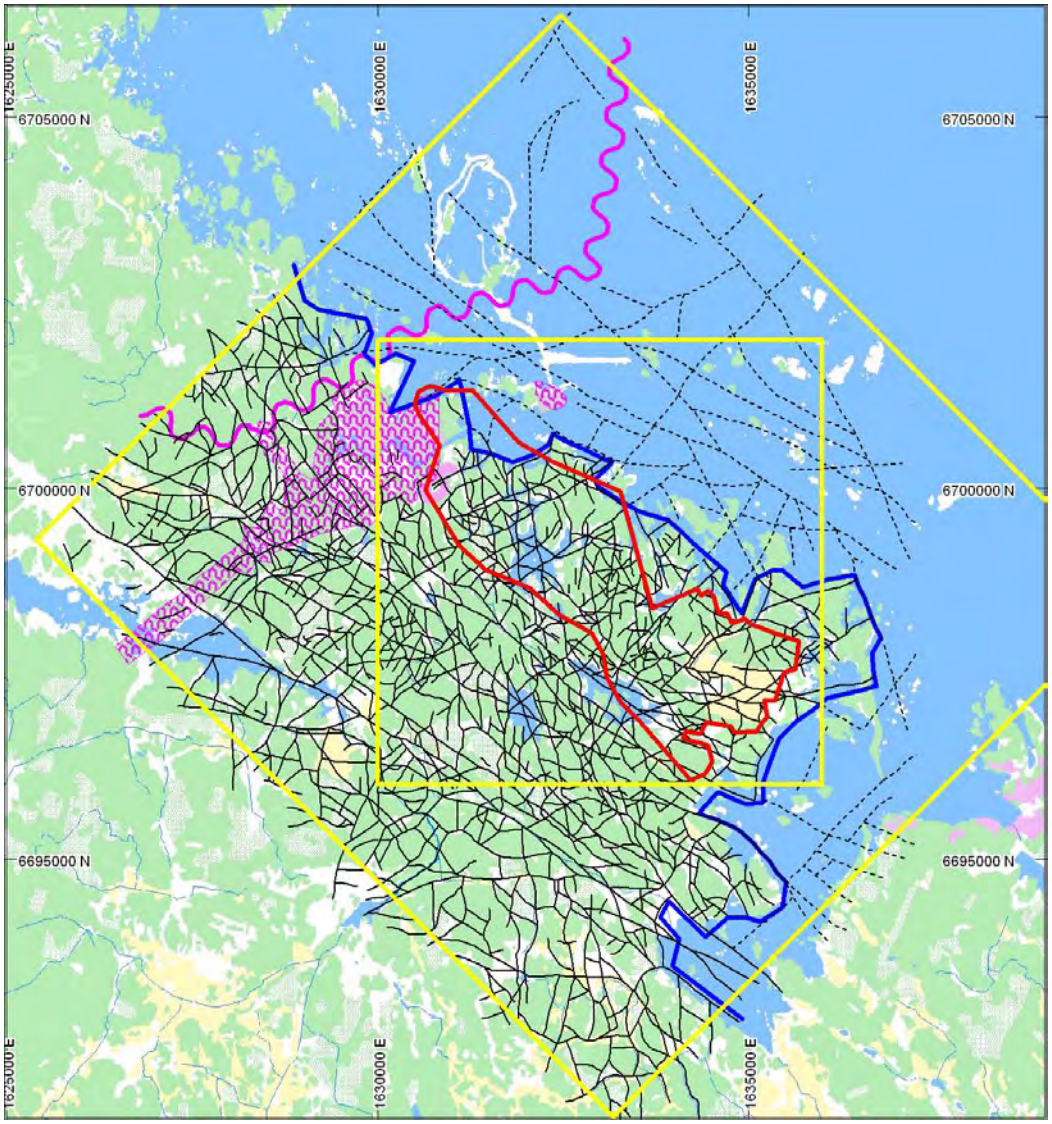


***Figure 5-4.*** *Coordinated lineaments on the mainland as solid black lines. Coordinated lineaments at sea, corresponding to magnetic lineaments, as dashed black lines. Solid blue line shows the boundary between the two classes. Forsmark candidate area is outlined with a red line. Yellow markers outline airborne survey areas. Magenta markers outline artificially disturbed areas.*

**Table 5-1. Compilation of some attribute information for coordinated lineaments. Figures give number of occurrences, except for "Average length" in metre.**

| Coordinated lineament | Low uncertainty | Medium uncertainty | High uncertainty | Total number | Average length (metre) | | |
|---|---|---|---|---|---|---|---|
| Total | 411 | 702 | 258 | 1371 | 373 | | |
| **Consists of: Method** | **Low uncertainty** | **Medium uncertainty** | **High uncertainty** | **Total number** | **Average length (metre)** | **1:st rank in combination with other methods** | **Solely one method** |
| Topography | 372 | 633 | 138 | 1143 | 356 | 327 | 628 |
| Magnetics | 216 | 186 | 122 | 524 | 486 | 119 | 119 |
| EM | 157 | 124 | 45 | 326 | 414 | 94 | 57 |
| VLF | 94 | 45 | 10 | 149 | 460 | 13 | 14 |
| ❖ EM and/or VLF (that is; conductivity) | 197 | 151 | 54 | 402 | 411 | 107 | 71 |
| Magnetics in the sea area | 18 | 29 | 35 | 82 | ➢ N/A | N/A | N/A* |

* Applicable if the airborne EM and VLF methods are considered to represent a common property; conductivity.

➢ N/A = not applicable

**Table 5-2. Attribute table for the coordinated lineaments.**

| Field name | Name | Description | Attribute used to describe coordinated lineaments |
|---|---|---|---|
| Id_t | Identity | Identity of the coordinated lineament | Not assigned in this work |
| Origin_t | Origin | Major type of basic data | Method specific lineaments |
| Class_t | Classification | Classification of the coordinated lineament | Not assigned in this work |
| Method_t | Method | The type of data in which the observation is identified | Magnetic,EM, VLF and/or elevation 10m grid; "magn,EM,VLF,topo" |
| Char_t | Character | Character of the observation | Coordinated lineament |
| Uncert_t | Uncertainty | Gradation of identification, in terms of uncertainty | Low/Medium/High |
| Comment_t | Comment | Specific comments to the observation | |
| Process_t | Processing | Data processing performed | image analysis, GIS |
| Date_t | Date | Point of time for interpretation | 20030411 |
| Scale_t | Scale | Scale of interpretation | 10000–20000 |
| Platform_t | Platform | Measuring platform for the basic data | Airborne geophysics 50m altitude, air photos from 2300 m altitude |
| Width_t | Width | Width on average | Not assigned in this work |
| Precis_t | Precision | Spatial uncertainty of position | 10–100m, 20m in general |
| Sign_t | Signature | Work performed by | hi (Hans Isaksson), GeoVista AB |
| Length_n | Length | Length of coordinated lineament | |
| Direct_n | Direction | Direction of coordinated lineament | |

In the sea area, where the coordinated lineaments are represented by a copy of the magnetic lineaments, the attribute table is the same as for magnetic lineaments, see Table 4-3.

### *Uncertainties*

The most important lack of balance in the coordination of method specific lineaments is that the interpretation of topographic lineaments has given information in much more detail then the interpretation of the airborne geophysics. The result is a large number of coordinated lineaments with only a topographic appearance, in this case 628 out of 1371 or 46%.

# 6 Linked lineaments

For the safety analysis of the site, the length of a fracture zone is important. However, the length calculated for a coordinated lineament does not give a good estimate and hence, it was judged necessary to link the various segments along what is judged with confidence to be the same lineament. For this reason, a specific methodology to link the coordinated lineaments was developed in cooperation with the project group for the Forsmark site description model, version 1.1. The linked lineaments obtained by this procedure then form a basis for identification of fracture zones in the bedrock and will also be used in the future site descriptive models.

The following data was used as input to the linking lineament procedure:

- coordinated lineaments on the mainland,
- coordinated magnetic lineaments in the sea area,
- in the NE part of the regional model area /5/, which is not covered by the new airborne geophysical survey, lineaments from site descriptive model, version 0 were used /5/.

## 6.1 Linking lineament procedure

The linking procedure called for preparation of some new attributes to facilitate the work.

A new weight attribute was created using a weighting scheme that depends on the degree of uncertainty and the number of methods, or in reality physical properties, used to identify each coordinated lineament, Table 6-1. A lineament identified in either VLF or EM is then considered to originate from a common property in the ground, that is, conductivity. Note that no property (method) has been given a higher weight in this scheme.

Results from a lineament trend analysis also provided some help to make priorities in the linking process /Jan Hermansson, oral communication/. The coordinated lineaments were divided in four direction sets and priorities; NW, NE, NS and EW, with the following critical angles:

- NW: 110–155° and 290–335°
- NE: 20–80° and 200–260°
- NS: 335–20° and 155–200°
- EW: 80–110° and 260–290°

**Table 6-1. Weighting scheme for linked lineaments.**

| Number of indicating properties (methods) | High uncertainty | Medium uncertainty | Low uncertainty |
|---|---|---|---|
| **3** of magnetics, topographic and conductivity | **3** | **4** | **5** |
| **2** of magnetics, topographic and conductivity | **2** | **3** | **4** |
| **1** of magnetics, topographic and conductivity | **1** | **2** | **3** |

The weight attributes and the trend was used as guidance how to link the different coordinated lineament segments together. To connect the different vector segments, this work also involved some minor adjustment of the node locations. Figure 6-1 shows an example of linking of lineaments.

To the “linked lineaments”, the most important new attributes assigned are:

- Identity. Each linked lineament is given identification according to SKB standards.
- Class. The total length provides a possibility to discriminate between regional (>10 km), local major (1–10 km) and local minor (<1 km) lineaments.

a) b)

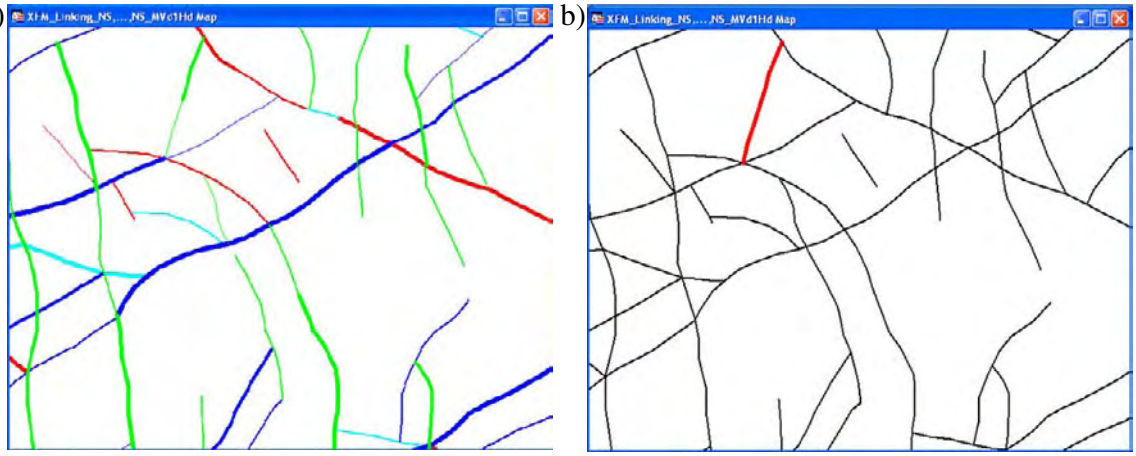

c)

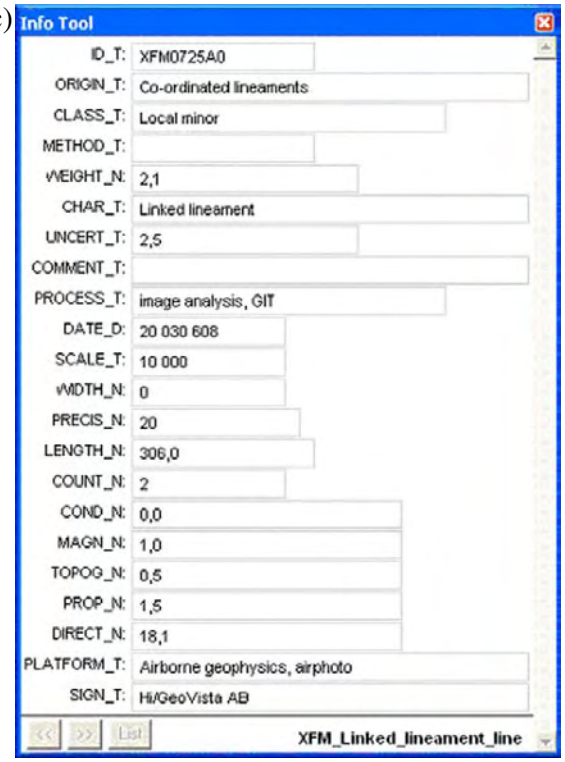


***Figure 6-1.*** *An example of lineament linking. a). Coordinated lineaments; NW, NE, NS and EW lineament trends in red, blue, green and cyan respectively. The line thickness is given according to the calculated weight. b). The same area after lineament linking. c). The attribute table for the red lineament marked in b).*

- Weight. The combination of uncertainty and number of properties (methods).
- Count. The number of original segments along the linked lineament.
- Cond, Magn, Topo. How much of the linked lineament that has been identified by the specific property (method), that is, conductivity, magnetics, topography.
- Uncertainty. Here the uncertainty is graded in figures; as 1=low, 2=medium and 3=high.

The attributes like Weight, Uncertainty, Cond, Magn and Topo are all weighted according to the length of each individual lineament that forms part of the total, linked lineament.

The interpretation results are stored in GIS-format and each unit has an attribute table attached, for full descriptions see also Table 6-2.

**Table 6-2. Attribute table for the linked lineaments.**

| Field name | Name | Description | Attribute used to describe linked lineaments |
|---|---|---|---|
| Id_t | Identity | Identity of the coordinated lineament | ID-number according to SKB's recom mendations (XFM……) |
| Origin_t | Origin | Major type of basic data | Coordinated lineaments, coordinated magnetic, Version 0 |
| Class_t | Classification | Classification of the coordinated lineament | Regional (>10 km), local major (1–10 km) and local minor (<1 km) lineaments. |
| Method_t | Method | The type of data in which the observation is identified | Not assigned in this work |
| Weight_n | Weight | A combination of uncertainty and number of properties (methods). An overall assessment of the quality of the linked lineament. This assessment is based on both the number of properties upon which the lineament has been identified and the degree of uncertainty. | A weighted average, graded continuously from 1=low quality to 5 =high quality, has been calculated, according to the length of each segment in the linked lineament. |
| Char_t | Character | Character of the observation | Linked lineament |
| Uncert_t | Uncertainty | Gradation of identification, in terms of uncertainty. In effect, this attribute is an expert judgement concerning the degree of clarity of the lineament. | An estimate of uncertainty of the linked lineament, graded as 1=low, 2=medium and 3=high. A weighted average has been calculated according to the length of each segment in the linked lineament. |
| Comment_t | Comment | Specific comments to the observation | |
| Process_t | Processing | Data processing performed | image analysis, GIS |
| Date_t | Date | Point of time for interpretation | 20030608 |
| Scale_t | Scale | Scale of interpretation | 10000–20000 |
| Width_t | Width | Width on average | Not assigned in this work |
| Precis_t | Precision | Spatial uncertainty of position. An estimate of how well the linked lineament is defined in space. | 10–100m, 20m in general |
| Count_n | Count | The number of original segments along the linked lineament. | integer |
| Cond_n | Conductivity | Shows how much of the linked lineament that has been identified by EM and/or VLF. | A weighted average has been calculated, according to the length of each segment in the linked lineament. 0.0–1.0 = 0–100% |

| Field name | Name | Description | Attribute used to describe linked lineaments |
|---|---|---|---|
| Magn_n | Magnetic | Shows how much of the linked lineament that has been identified by magnetics. | A weighted average has been calculated, according to the length of each segment in the linked lineament.<br>0.0–1.0 = 0–100% |
| Topo_n | Topography | Shows how much of the linked lineament that has been identified by topography. | A weighted average has been calculated, according to the length of each segment in the linked lineament.<br>0.0–1.0 = 0–100% |
| Prop_n | Property | Shows in average, how many properties that has been identified the linked lineament | A weighted average has been calculated, according to the length of each segment in the linked lineament.<br>0.0–1.0 = 0–100% |
| Length_n | Length | The length of the linked lineament | |
| Direct_n | Direction | The average trend of the linked lineament | 0–360 degrees |
| Platform_t | Platform | Measuring platform for the basic data | Airborne geophysics 50m altitude, air photos from 2300 m altitude |
| Sign_t | Signature | Work performed by | hi (Hans Isaksson), GeoVista AB |

## 6.2 Linked lineament results

In total, 879 linked lineaments have been defined; of which 851 lineaments have a unique identity name (first 7 positions of the identity code, XFMxxxx). This means that 28 lineaments forms separate segments of what is judged with confidence to be part of the same lineament as mentioned above. These segment lineaments have different denomination in position 8–9 in the identity code. The ground for this special treatment is that the separate segments 1) form alternative routes for regional or local major lineaments or 2) are linked together from different input data, that is; coordinated, coordinated magnetic or version 0 lineament.

7 lineaments, totally 18 segments, are classified as regional lineaments (length > 10 km),
150 lineaments, totally 167 segments, are classified as local major (1–10 km), and
694 lineaments are classified as local minor lineaments (< 1 km).

The average length of all lineaments and the adherent segments are 794 m.

94 lineaments have a weight of 4 or higher
187 lineaments have a weight between 3 and 4,
416 lineaments have a weight of 2 to 3, and
161 lineaments have a weight below 2.

Finally 21 lineaments originating from version 0 model have a weight of 0 and lacks information on other attributes as well.

116 lineaments have been observed in all three properties,
46 lineaments are only observed in conductivity, that is, EM and/or VLF,
89 lineaments are identified only in magnetics, and
400 lineaments are identified only in topography.

At sea, the lineaments are, beside version 0 lineaments, represented by a copy of the interpretation of magnetic lineaments and hence, the attribute table is not complete.

The comprehensive attributes table is built up to provide a basis for further statistical analysis and scrutiny of the linked lineaments as possible fracture zones.

A figure of the linked lineaments is not presented here, since it will give a very similar picture as Figure 5-4 showing the coordinated lineaments. However, a selection of linked lineaments, classified as regional or local major (longer then 1 km) is presented in Figure 6-2.

#### *Uncertainties*

In some cases, more than one way to link two coordinated lineaments is possible. How the linking is done might then also affect the length of the linked lineament.

Several of the lineaments are not terminated, but have an open end at the interpretation boundary. Consequently these lineaments are given a minimum length.

In this version, lineaments have not been cut when crossing regional fracture zones like the Singö zone and the Forsmark zone /5/. Such decisions will need more information or other presumptions as a part of the analysis work.

In some cases, a lineament with low uncertainty over a long length can have an uncertain but short link between the longer segments. This information is not valued in this methodology. The weighted average according to the length of each segment will give this possible break a very low significance.

## 6.3 Upgrading lineaments to fracture zones

The final phase in the lineament integration comprises a possibility to upgrade a linked lineament to a fracture zone. This decision is based on surface geological data, detailed ground geophysics and/or other ground truth data. In cooperation with Mike B Stephens and Jan Hermansson (members of the project group for site descriptive modelling), a few lineaments were upgraded to fracture zones as an initial basis for the subsequent work for model version 1.1.

In total 10 lineaments and related segments were upgraded to fracture zones, of which one also shows kinematic indications. The basis for the upgrading was outcrop data, refraction seismics and geological information from the construction of the Forsmark nuclear power plants and SFR.

It should be noted that this work was only preliminary and was further continued in more detail within the work for the site descriptive model version 1.1. Hence, the results are not further discussed in this report.

Figure 6-2 shows linked lineaments longer than 1 km and lineaments upgraded to fracture zones.

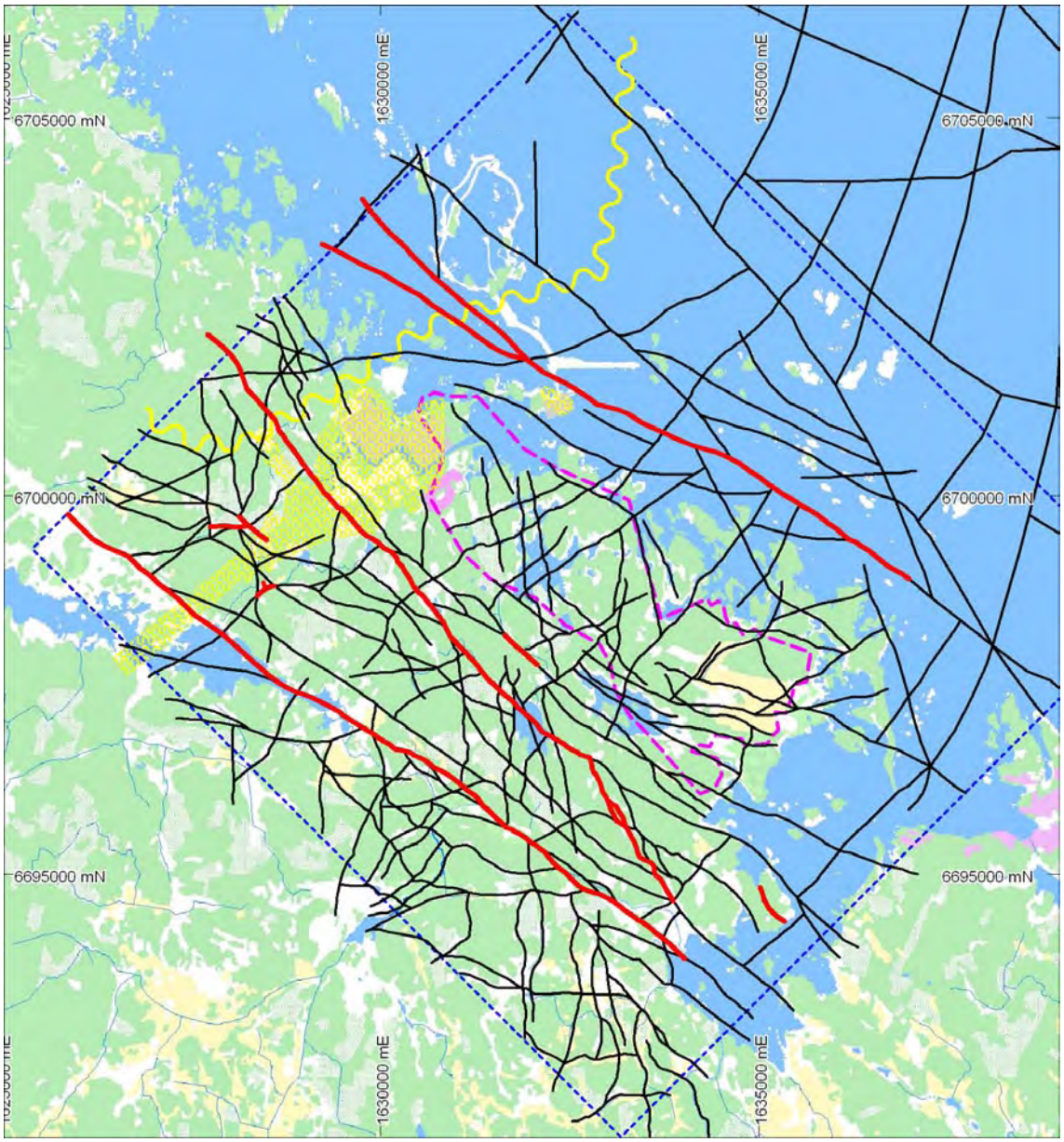


***Figure 6-2.*** *Linked lineaments, regional and local major (length > 1 km) are shown as solid black lines. Lineaments that have been upgraded to a fracture zone are shown as solid red lines. The Forsmark candidate area is outlined with magenta dashed line. Disturbed areas are outlined in yellow and the boundary for the helicopter borne geophysical survey is outlined by a blue dashed line.*

# 7 Work flow for integrated lineament interpretation, summary

The main purpose of the lineament interpretation is to identify linear features that can indicate possible deformation zones in the bedrock. The method of lineament interpretation follows several distinct phases.

Phase I has included interpretation of each method (topography, magnetics, VLF and EM) separately and each “method specific lineament” has been given a set of attribute data, of which the most important are; origin, character, precision and an assessment of clarity in terms of low, medium and high uncertainty.

Phase II has included coordination of the method specific lineaments into “coordinated lineaments” and the discriminating methods for each lineament are added as attribute data.

In phase III, the coordinated lineaments are linked together spatially. A new weight attribute is created using a weighting scheme that depends on the degree of uncertainty and the number of properties (methods) used to identify each coordinated lineament. Results from a lineament direction analysis provided help to make priorities in the linking process. In the “linked lineaments”, the attributes such as uncertainty, the combination of uncertainty and number of methods, and the basis for interpretation, are all weighted according to the length of each individual lineament that forms part of the linked lineament. The total length provides a possibility to discriminate between regional (>10 km), local major (1–10 km) and local minor (<1 km) lineaments, and this classification is placed in a new attribute field. Each linked lineament is given identification according to SKB standards. The comprehensive attributes table facilitates further statistical analysis and scrutiny of the linked lineaments as possible fracture zones.

Finally, based on surface geological data, detailed ground geophysics and/or other ground truth data, some lineaments or parts of a lineament can be upgraded to a fracture zone (phase IV).

Figure 7-1, summarizes the work for integrated lineament interpretation in a flowchart.

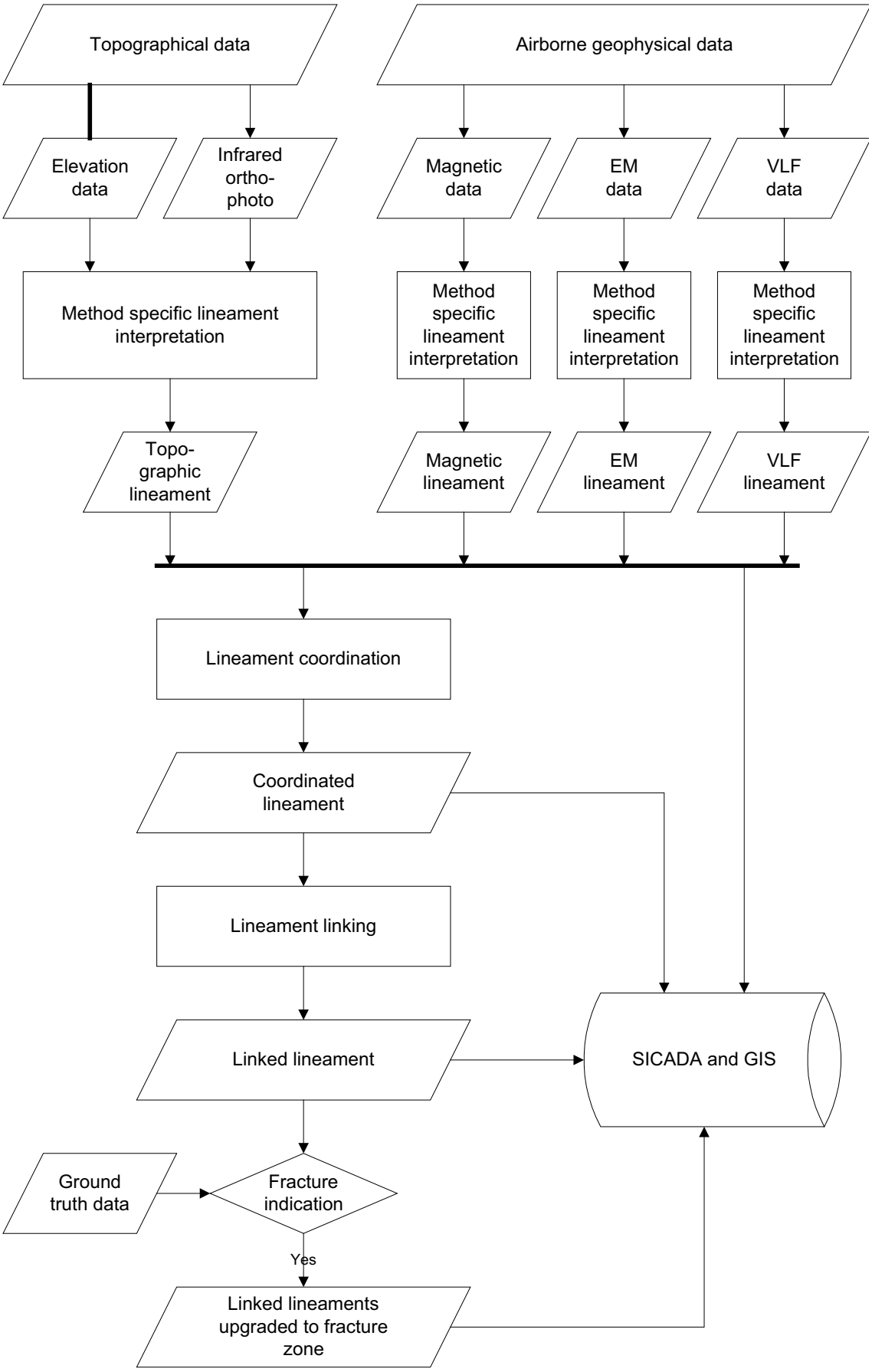


***Figure 7-1.*** *Flowchart for integrated lineament interpretation.*

# 8 Data delivery

The processed data and interpretation results have been delivered to SKB as described below. The SICADA field note number is Forsmark No 117. All GIS data have been documented according to “GIS – Inleverans av data”, SKB SD-081.

Data have been delivered in three data formats for storage in the GIS-database. Files that show post-processed grid-files have been delivered as georeferenced tiff-pictures and also used in the creation of figures to the report. Information that has resulted in some kind of interpreted vector; point, line or polygon information has been stored in Shape format. One file with airborne magnetic data from SGU has been delivered as a grid-file. A listing of delivered products is found in Appendix 1.

# 9 References


**/1/ Munier R, Stanfors R, Milnes A G, Hermansson J, Triumf C-A, 2003.** Geological site descriptive model. A strategy for the model development during site investigations. SKB R-03-07.

**/2/ Mattsson H, Isaksson H, Thunehed H, 2003.** Petrophysical rock sampling, measurements of petrophysical rock parameters and in situ gamma ray spectrometry measurements on outcrops carried out 2002. SKB P-03-26.

**/3/ Isaksson H, Mattsson H, Thunehed H, Keisu M, 2004.** Interpretation of petrophysical surface data. Stage 1 (2002). SKB P-03-102.

**/4/ Bergman S, Bergman T, Isaksson H, Johansson R, 1998.** Förstudie Östhammar. Delprojekt jordarter, bergarter och deformationszoner. Kompletterande arbeten 1998. SKB R-03-07.

**/5/ SKB, 2002.** Forsmark – site descriptive model version 0. SKB R-02-32.

**/6/ Rönning H J S, Kihle O, Mogaard J O, Walker P, Shomali H, Hagthorpe P, Byström S, Lindberg H, Thunehed H, 2003.** Forsmark site investigation. Helicopter borne geophysics at Forsmark, Östhammar, Sweden. SKB P-03-41.

**/7/ Shomali H, Hagthorpe P, Byström S, 2002.** Removal of DC power line influence on magnetic data in the Forsmark area. In Forsmark site investigation. Helicopter borne geophysics at Forsmark, Östhammar, Sweden. SKB P-03-41. /6/.

**/8/ Duda and Hart, 1973.** Pattern Classification and Scene Analysis, John Wiley and Sons, chapter 2.

**/9/ Schowengerdt R A, 1983.** Techniques for Image Processing and Classification in Remote Sensing. Academic Press.

**/10/ Isaksson H, 2003.** Interpretation of topographic lineaments 2002. SKB P-03-40.

**Jan Hermansson, oral communication.**

**Sören Byström, SGU, oral communication.**

# Appendix 1

## Delivered data

### Shape-files

| Filename | Filetype | Information type | Content |
|---|---|---|---|
| XFM_Co-ordinated_line | Shape | Co-ordinated lineaments | Co-ordinated lineaments interpreted from airborne geophysics (magnetics, EM and VLF) and topography, only mainland |
| XFM_Co-ordinated_Magnetic_line | Shape | Co-ordinated lineaments | "Co-ordinated" magnetic lineaments interpreted from airborne magnetics ONLY. Valid to the Sea area. |
| FM_Sea_lineament_boundary_line | Shape | | Sea lineament boundary that defines the area for which the co-ordinated lineament interpretation has been performed |
| FM_Disturbed_Area_polygon | Shape | Disturbed area | Disturbed areas for interpretation of airborne geophysics, usually powerlines, Forsmark power plant and distribution plant, DC-cable and DC-cable station |
| FM_Fracture zone_Kinematics_line | Shape | Fracture zone | Fracture zones delineated from geological observations, refraction seismic and co-ordinated lineaments interpreted from airborne geophysics (magnetics, EM and VLF) and topography. Kinematics are noted. |
| FM_Fracture zone_line | Shape | Fracture zone | Fracture zones delineated from geological observations, refraction seismic and co-ordinated lineaments interpreted from airborne geophysics (magnetics, EM and VLF) and topography |
| FM_Magnetic_connections_line | Shape | Magnetic connections | Connections of magnetic maximas interpreted from airborne magnetics |
| FM_Magnetic_High_line | Shape | Magnetic highs | Connections of magnetic high anomalies interpreted from airborne magnetics |
| FM_Magnetic_High_polygon | Shape | Magnetic highs | Connections of magnetic high anomalies interpreted from airborne magnetics |
| FM_Magnetic_pattern_polygon | Shape | Magnetic patterns | Magnetic pattern areas interpreted from airborne magnetics |
| XFM_Magnetic_line | Shape | Magnetic lineament | Magnetic lineaments interpreted from airborne magnetics, usually magnetic minimas |
| XFM_vlf_line | Shape | Electromagnetic lineaments | Lineaments interpreted from helicopter-borne VLF survey. |
| XFM_em_line | Shape | VLF lineaments | Lineaments interpreted from helicopter-borne EM survey. |
| FM_Gamma-ray_spectrometry_classification_polygon | Shape | Gamma-ray spectrometry classification | Airborne gamma-ray spectrometry, maximum likelihood classification |
| FM_Class_probability-50%_polygon | Shape | Class probability | Areas with low probability (< 50%) to belong to the settled class |
| FM_Classified_area_polygon | Shape | Classified area | Area describing the classfied area |
| FM_Training_areas_polygon | Shape | Traning area | Training areas for the maximum likelihood classification of the airborne gamma-ray spectrometry |
| XFM_linked_lineament_line | Shape | Linked lineaments | Linked lineaments from co-ordinated, co-ordinated magnetic and version 0 lineaments |

## Grid- and xls-files

| Filename | Filetype | Information type | Content |
|---|---|---|---|
| FM_TIEM_2003 | Grid | Magnetic | Mosaic created from airborne magnetical data from SGU with cultural anomaly removed. |
| **Filename** | **Filetype** | **Information type** | **Content** |
| Gammaspek_Site-mean | xls | Spectrometry | Site average on K, U and Th, calculated for each outcrop and rocktype |

## Tiff-files

| Filename | Filetype | Information type | Content |
|---|---|---|---|
| EW_Magn_Vd1 | Tiff | Magnetic, grayscale | Vertical derivative of magnetic total field |
| NS_Magn_Vd1 | Tiff | Magnetic, grayscale | Vertical derivative of magnetic total field |
| EW_MVd1Hd | Tiff | Magnetic, RGB colour composite | Red,Green,Blue = Magnetic total field,Magnetic vertical derivative,Magnetic horisontal derivative |
| NS_MVd1Hd | Tiff | Magnetic, RGB colour composite | Red,Green,Blue = Magnetic total field,Magnetic vertical derivative,Magnetic horisontal derivative |
| FM_TieM_2003_MVd1Hd | Tiff | Magnetic, RGB colour composite | Airborne magnetics, edited, presented as a RGB colour composite of magnetic total field ®, 1:st vertical detivative (G) and horizontal derivative (B). |
| APPRESQ2LOG | Tiff | EM | Transformed data from NS-flightlines, coplanar coils. |
| APPRESQ2LOG_LEG | Tiff | EM | Legend (color scale), log10(rho-a) [Ohm-m] |
| APPRESQ5LOG | Tiff | EM | Transformed data from NS-flightlines, coplanar coils. |
| APPRESQ5LOG_LEG | Tiff | EM | Legend (color scale), log10(rho-a) [Ohm-m] |
| IP1EWAGC | Tiff | EM | Filtered data from EW-flight lines, coaxial coils |
| IP1NSAGC | Tiff | EM | Filtered data from NS-flight lines, coaxial coils |
| IP2EWAGC | Tiff | EM | Filtered data from EW-flight lines, coplanar coils |
| IP2NSAGC | Tiff | EM | Filtered data from NS-flight lines, coplanar coils |
| IP3EWAGC | Tiff | EM | Filtered data from EW-flight lines, coaxial coils |
| IP3NSAGC | Tiff | EM | Filtered data from NS-flight lines, coaxial coils |
| IP4EWAGC | Tiff | EM | Filtered data from EW-flight lines, coplanar coils |
| IP4NSAGC | Tiff | EM | Filtered data from NS-flight lines, coplanar coils |
| IP5EWAGC | Tiff | EM | Filtered data from EW-flight lines, coplanar coils |
| IP5NSAGC | Tiff | EM | Filtered data from NS-flight lines, coplanar coils |
| Q1EWAGC | Tiff | EM | Filtered data from EW-flight lines, coaxial coils |
| Q1NSAGC | Tiff | EM | Filtered data from NS-flight lines, coaxial coils |
| Q2EWAGC | Tiff | EM | Filtered data from EW-flight lines, coplanar coils |
| Q2NSAGC | Tiff | EM | Filtered data from NS-flight lines, coplanar coils |
| Q3EWAGC | Tiff | EM | Filtered data from EW-flight lines, coaxial coils |
| Q3NSAGC | Tiff | EM | Filtered data from NS-flight lines, coaxial coils |
| Q4EWAGC | Tiff | EM | Filtered data from EW-flight lines, coplanar coils |
| Q4NSAGC | Tiff | EM | Filtered data from NS-flight lines, coplanar coils |
| Q5EWAGC | Tiff | EM | Filtered data from EW-flight lines, coplanar coils |
| Q5NSAGC | Tiff | EM | Filtered data from NS-flight lines, coplanar coils |
| VLT_EW | Tiff | VLF | VLF-data from inline-sensor, EW flight lines |
| VLT_NS | Tiff | VLF | VLD-data from inline-sensor, NS flight lines |
| VOT_EW | Tiff | VLF | VLF-data from ortho-sensor, EW flight lines |
| VOT_NS | Tiff | VLF | VLF-data from ortho-sensor, NS flight lines |
| NSEW_Spek_ThKaUr | Tiff | Spectrometry, RGB colour composite | Natural gamma spectrometry, Red,Green,Blue = Th,Ka,Ur |